

EUROPEAN PROGRESS TOWARD NANOSTRUCTURE ENGINEERING IN COATED CONDUCTORS

A. Palau

Institut de Ciència de materials de Barcelona (ICMAB-CSIC), Barcelona, Spain

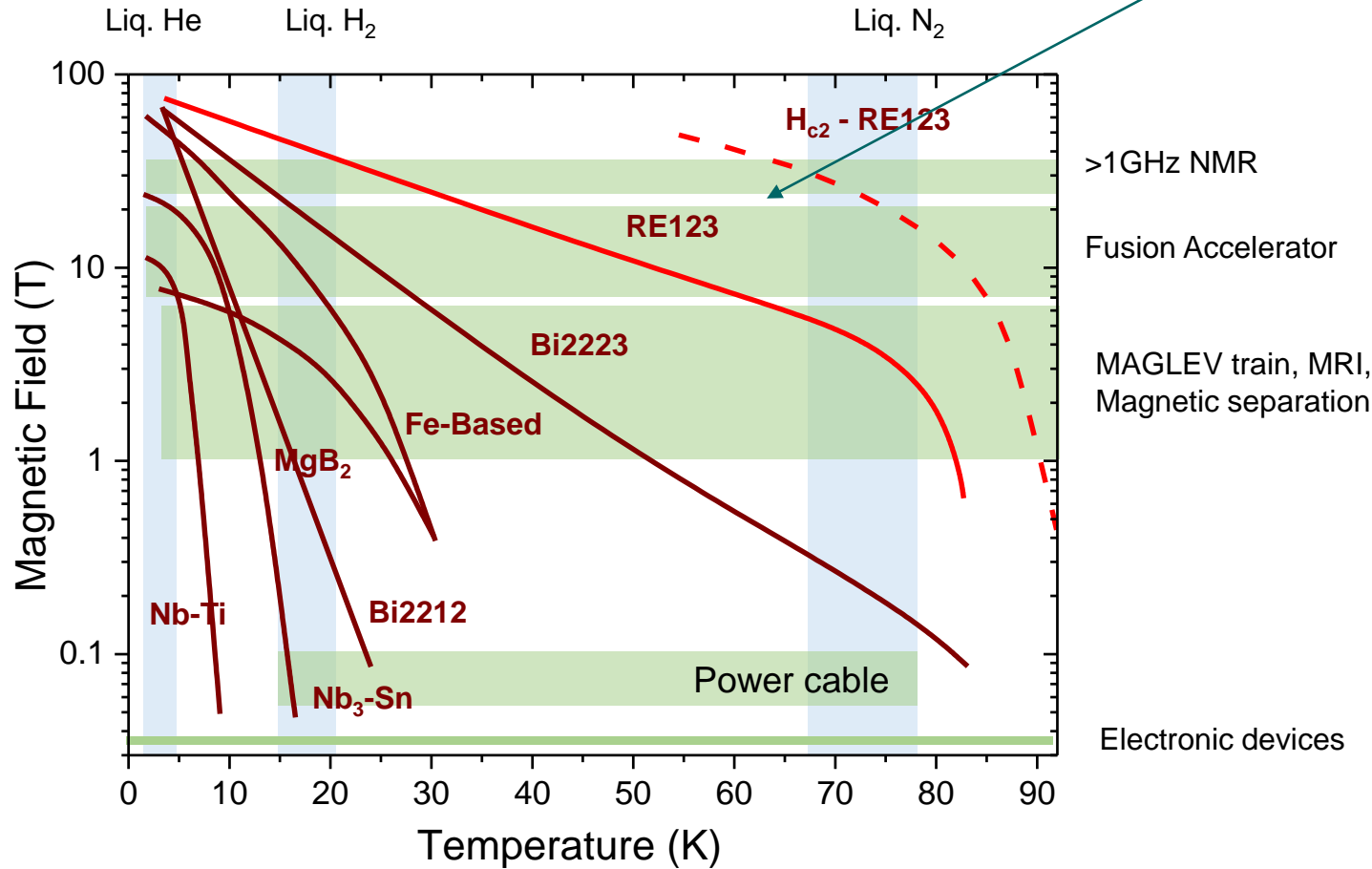
EUROTAPES collaborative project

(**E**uropean development of Superconducting **T**apes: integrating novel materials and architectures into cost effective processes for power applications and magnets)



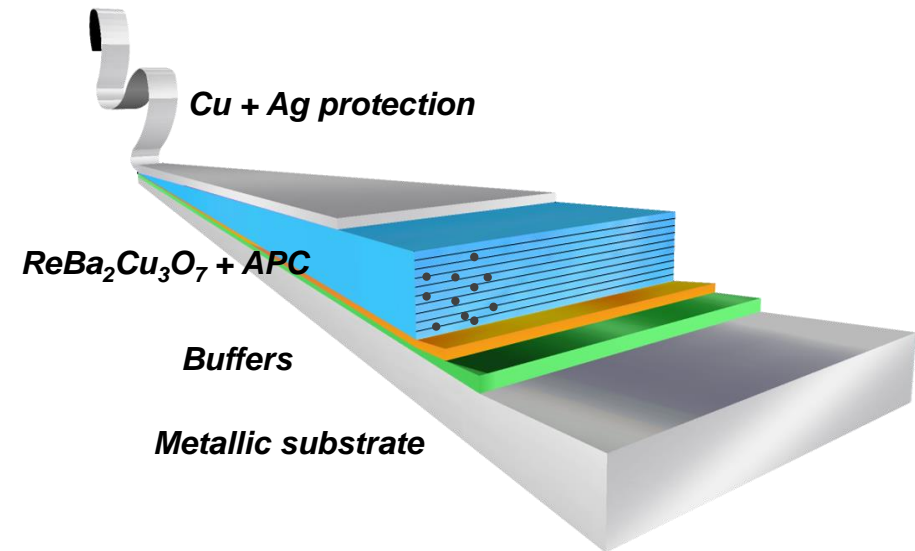
COATED CONDUCTORS: CHALLENGES AND OPPORTUNITIES

Nanotechnology engineering enables to improve ReBCO CC performance



Main Goal

Optimize the pinning centres according the specific working conditions (H, T) for CC applications

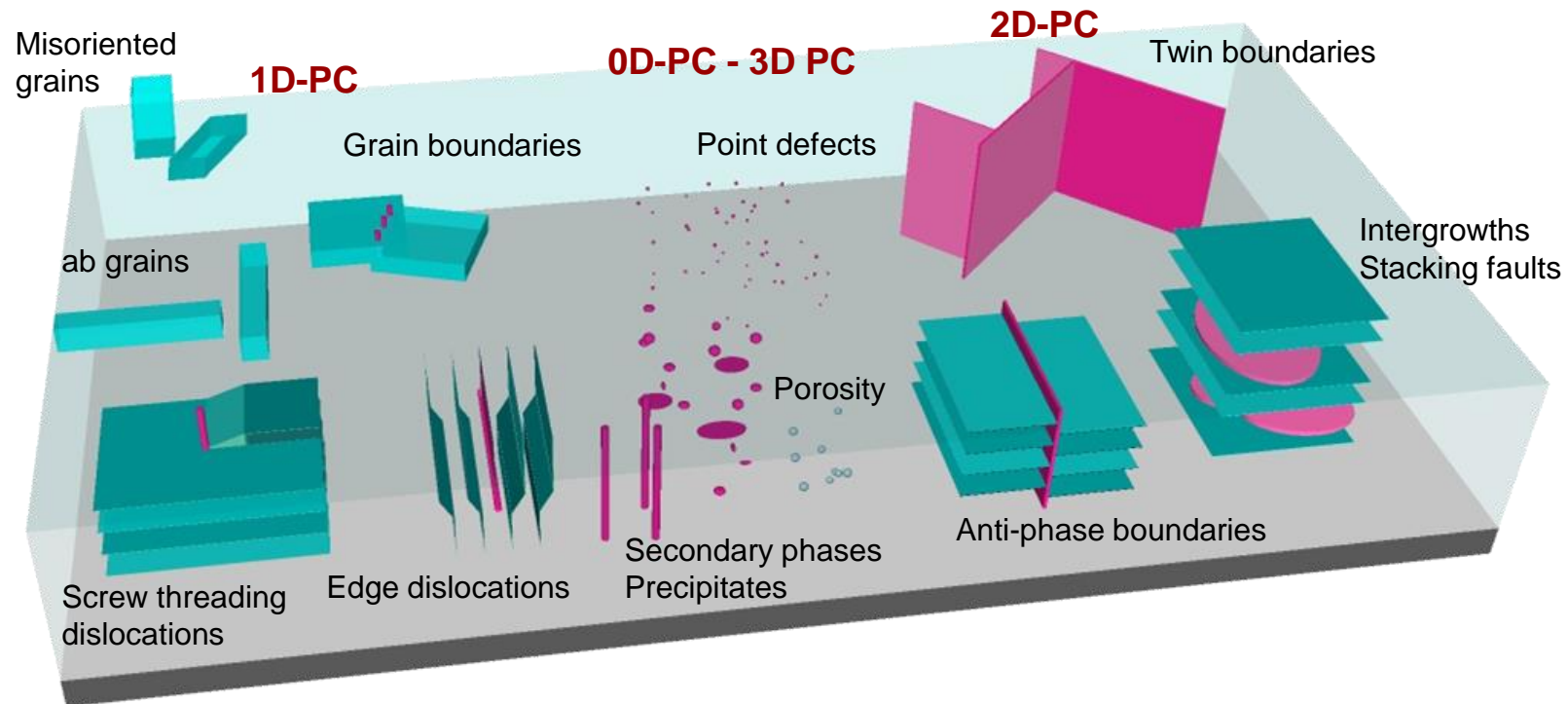


Applications requiring $J_e > 10^4 \text{ A cm}^2$ for various superconducting tapes and wires [Shimoyama, SUST 27 (2014)]

DESIGNING THE PINNING LANDSCAPE IN YBCO NANOCOMPOSITES

Nanocomposite YBCO films and CCs and their final **nano-structure** deeply differs depending on

- Growth technique \Rightarrow Simultaneous or deferred nucleation
 - Growth conditions (Rate, Temperature,...)
 - Chemistry of secondary phase (or mixed additions)
 - % addition
 - Substrate
- \Rightarrow
- Strain with the Matrix (Epitaxial or randomly)
 - Geometry (nano-rods, nano-particles,...)
 - Size, distribution
 - Shape / orientation (correlated, isotropic) / size / distribution



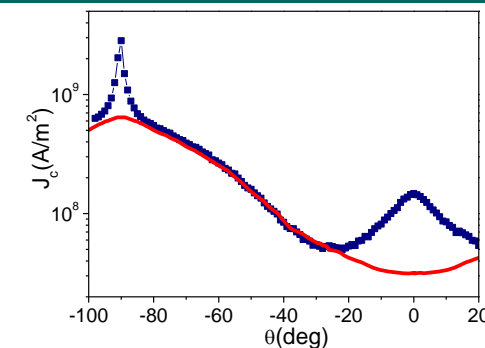
Superposition of different dimensionalities in a single material

VORTEX PINNING IN YBCO NANOCOMPOSITES: ANISOTROPY

In field angular $J_c(\theta)$ dependence

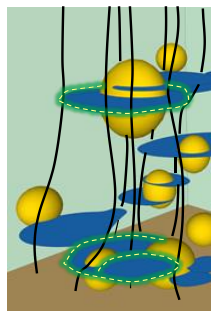
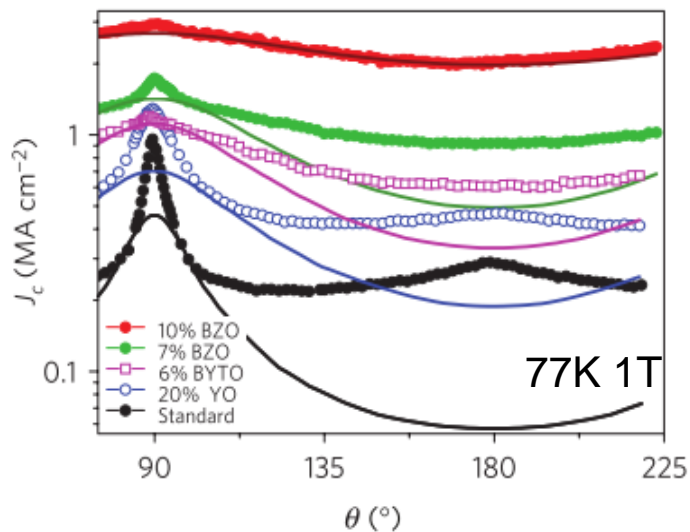
$$J_c = J_c^{H//c} (\sin^2\theta/\gamma^2 + \cos^2\theta)$$

Anisotropy of J_c in high H even at T is one of key issue



CSD Nanocomposites with random NP

Nanostrain \Rightarrow quasi-isotropic vortex-pinning with a highly reduced $\gamma_{\text{eff}} \sim 1.5 - 2$



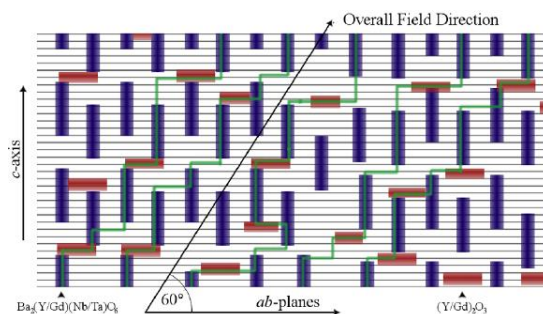
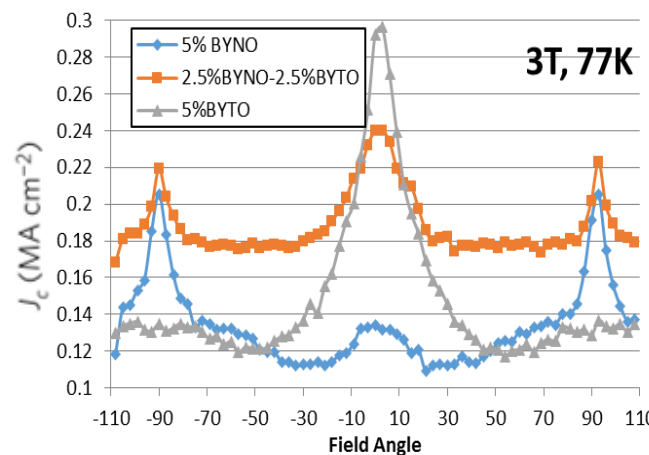
Llordes, Palau et al. Nat. Mat. 11 (2012)

PLD Nanocomposites \Rightarrow

Mixed Nanocomposites

Tuning the growing conditions

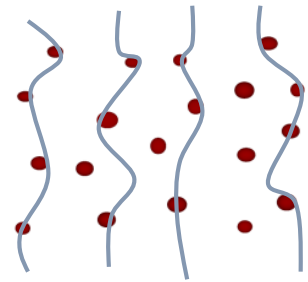
Combination of correlated defects along the c axis and ab-planes



Ercolano et al. SUST 24 (2011)

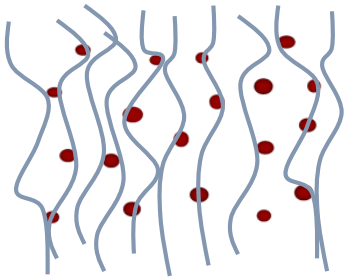
VORTEX PINNING IN YBCO NANOCOMPOSITES: FIELD DEPENDENCE

Magnetic Field $J_c(H)$ dependence



Single vortex pinning

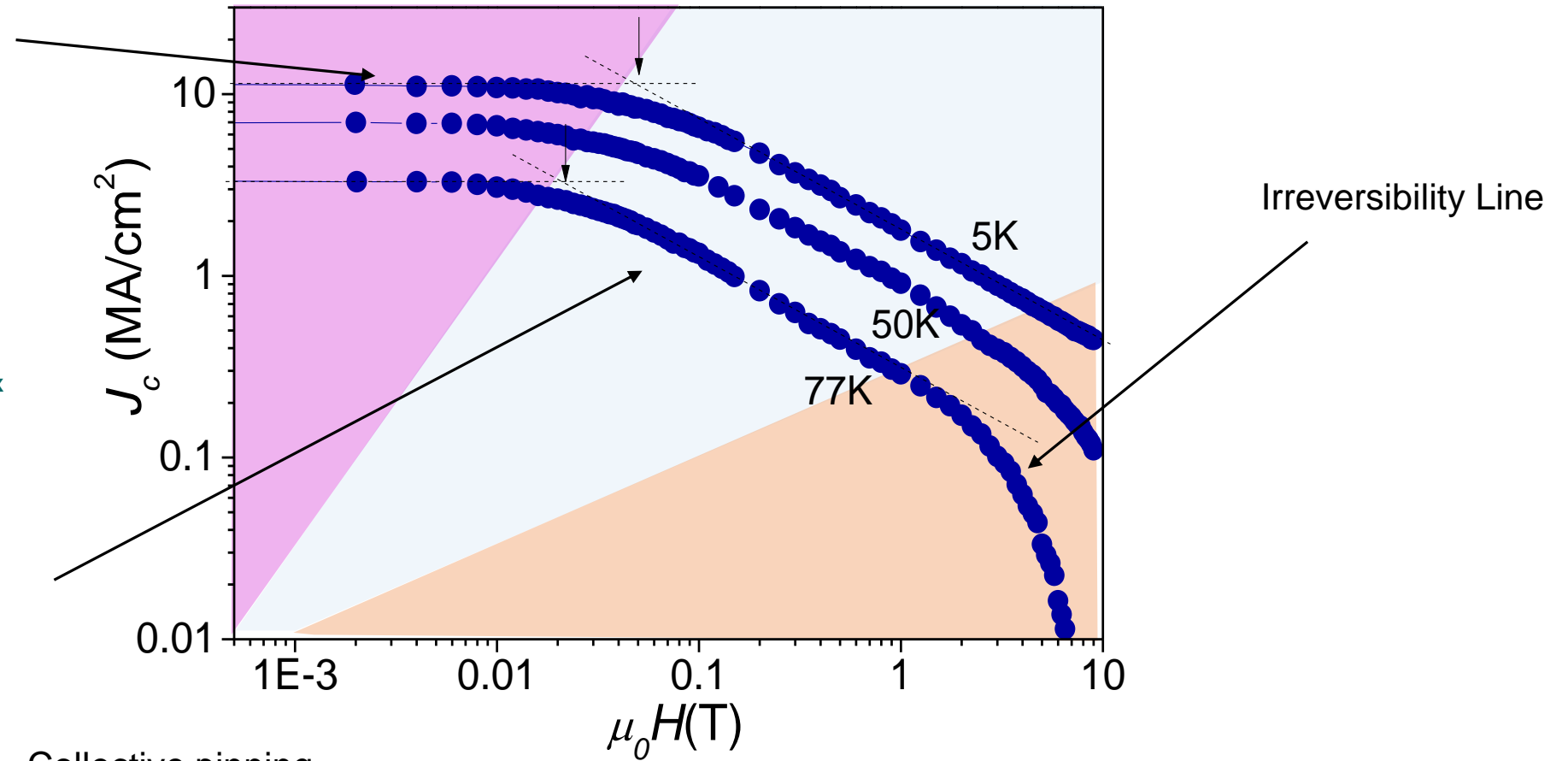
$$E_{\text{int}}^{\text{vortex-defect}} > E_{\text{int}}^{\text{vortex-vortex}}$$



Collective pinning

$$E_{\text{int}}^{\text{vortex-vortex}} \uparrow \uparrow$$

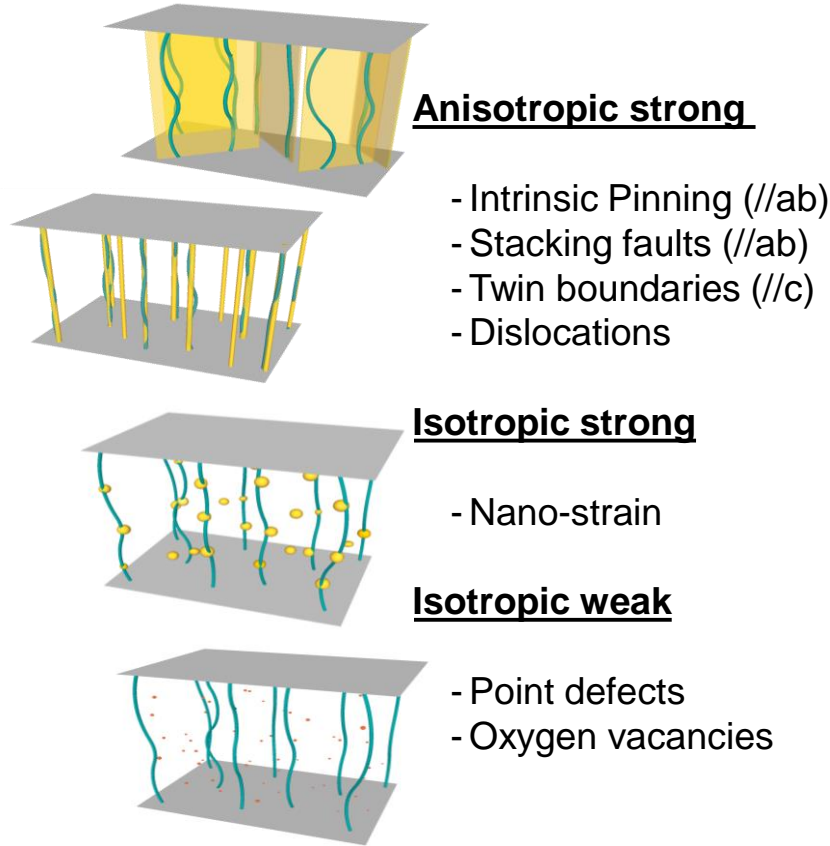
Different vortex pinning regimes



VORTEX PINNING IN YBCO NANOCOMPOSITES: TEMPERATURE DEPENDENCE

Temperature $J_c(T)$ dependence

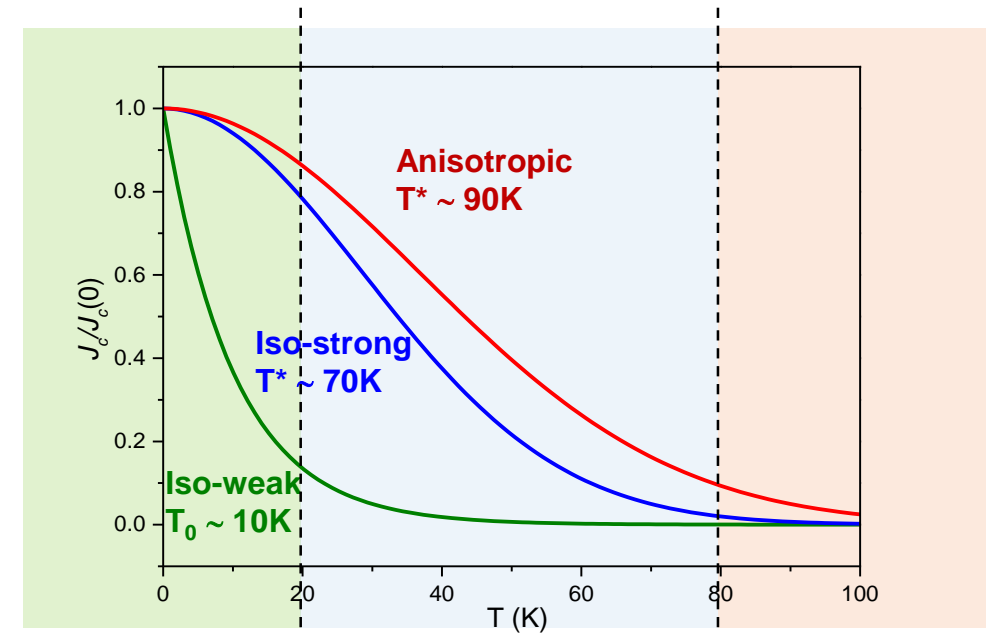
Vortex pinning efficiency at different field / temperatures can be correlated with the nanoscale defect structure.



$$J_c^{strong}(T) = J_c^{str}(0) \exp \left[-3 \left(\frac{T}{T^*} \right)^2 \right]$$

$$J_c^{weak}(T) = J_c^{wk}(0) \exp \left(-\frac{T}{T_0} \right)$$

characteristic vortex pinning energy for each defect



Quantify pinning strength and energies associated to different pinning centres

- $J_c^{str}(0), J_c^{wk}(0) \rightarrow$ strength, density of defects
- $T^*, T_0 \rightarrow$ thermal activation

All three contribute, Isotropic-weak has some relevance

Combination of anisotropic and Isotropic-strong

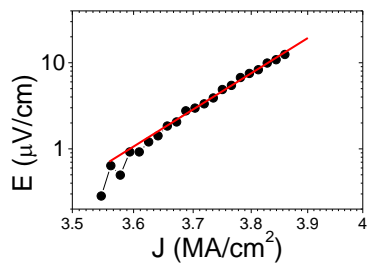
Anisotropic pinning becomes dominant

Blatter et al PRL 68 (1992), Civale, et al APL 84 (2004), Puig et al. SUST. 21 (2008)

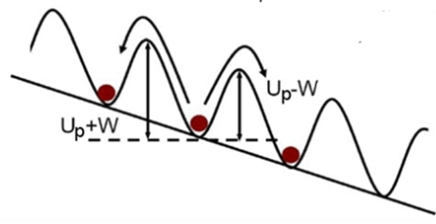
VORTEX DYNAMICS IN YBCO NANOCOMPOSITES: CREEP

Vortex Creep

Transport measurements

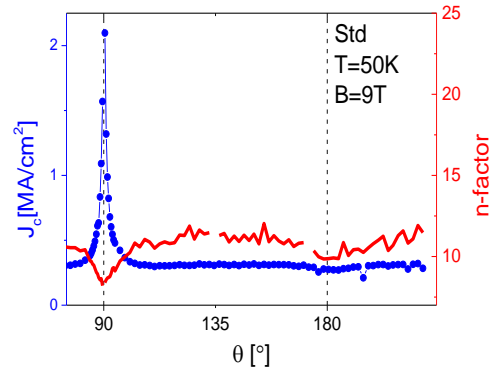
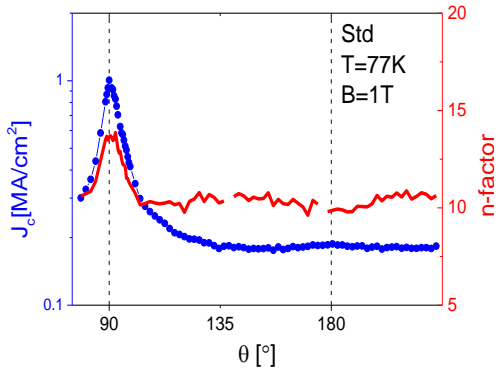


$$E \propto J^N \rightarrow N \sim U_p/kT$$

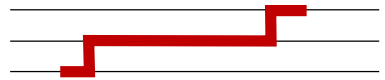


In general $N \propto J_c$

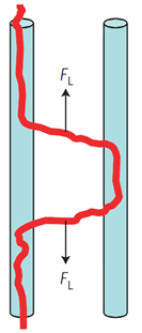
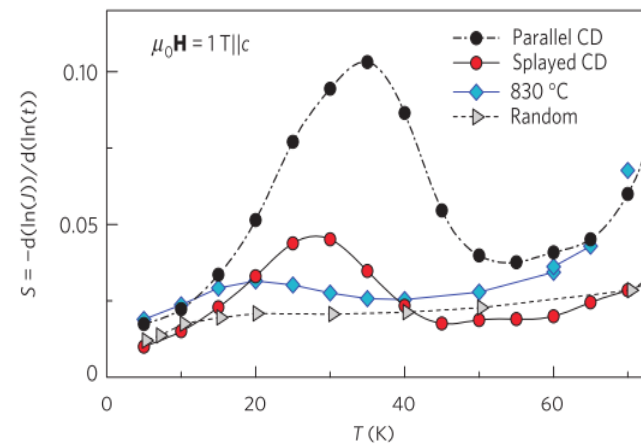
Inverse correlation $J_c \propto 1/N$ at $H//ab$ (intrinsic pinning)



Range where intrinsic pinning is dominant \Rightarrow Loss in U_p due to the formation of double kink excitations



Relaxation measurements



large peak in $S(T)$ observed in YBCO films with parallel columnar defects \Rightarrow easy expansion of double kinks between adjacent defects

Maierov et al. Nat Mat. 8 (2009)

Double King formation in correlated defects must be avoid

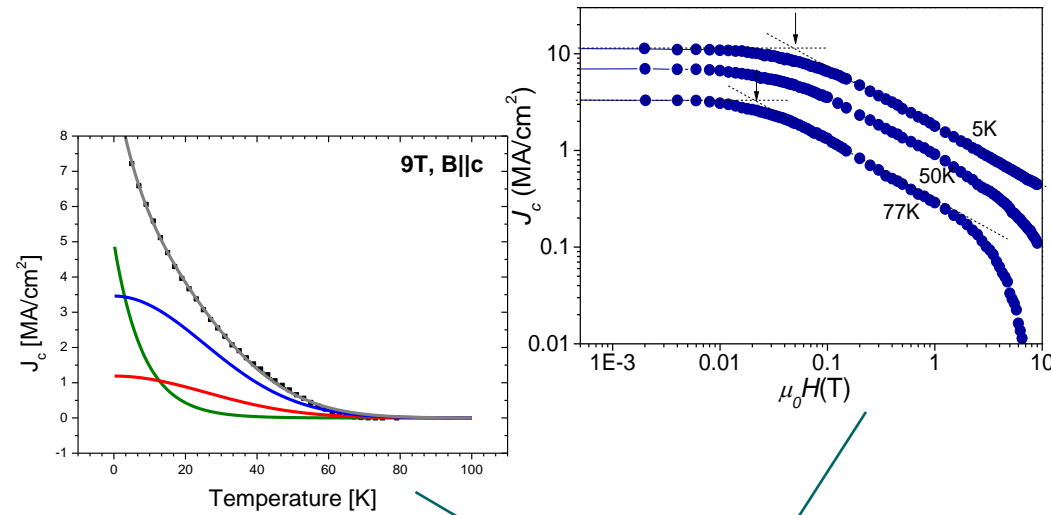
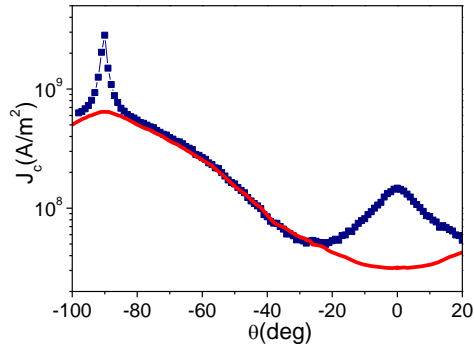
- $H//ab \Rightarrow$ Intrinsic pinning
- $H//c \Rightarrow$ straight correlated defects, twin boundaries

Blatter et al. RMP 66 (1994)

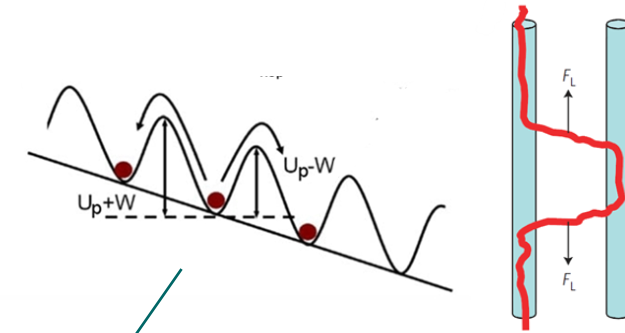
Civile et al. IEEE trans. Appl. Superc. 15 (2005)

DESIGNING THE VORTEX PINNING LANDSCAPE

Vortex Pinning Force (θ, H, T)



Vortex Creep

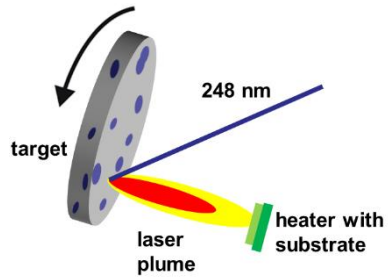


Defect structure must be engineered according to the operating H - T range and considering **vortex pinning & dynamics**

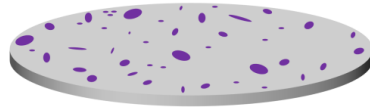
⇒ Mixed microstructure with synergetic vortex pinning centers may good for a wide range of temperature and field

REBCO NANOCOMPOSITES GROWN BY PLD

Simultaneous deposition and growth

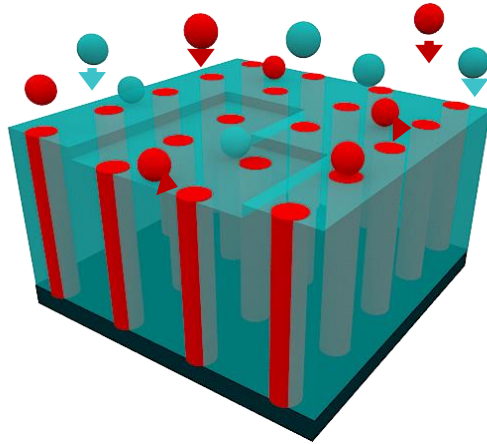


Self-assembled perovskites
 BaZrO_3 (BZO), BaHfO_3 (BHO), Ba_2YTaO_6 (BYTO) $\text{Ba}_2\text{Y}(\text{Nb}_{0.5}\text{Ta}_{0.5})\text{O}_6$ (BYNTO) ...



Mixed targets from stoichiometric powders

PLD, e-beam, MOCVD, HLPE

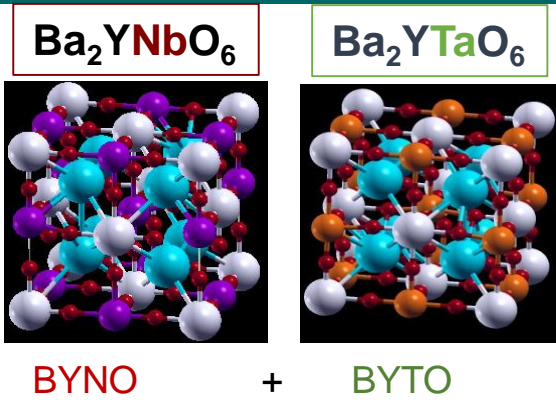


Self-assembled c axis oriented rods

- Simultaneous growth
- interfacial energies and strain
- diffusion length of the respective atomic species
- Temperature
- Grown Rate (i.e. laser repetition rate)
- growth direction (vicinality of the substrate)

Vortex pinning mostly ascribed to self-assembled secondary phases and associated interfacial strain

YBa₂Cu₃O_{7-x} + MIXED Ta / Nb BASED APCs



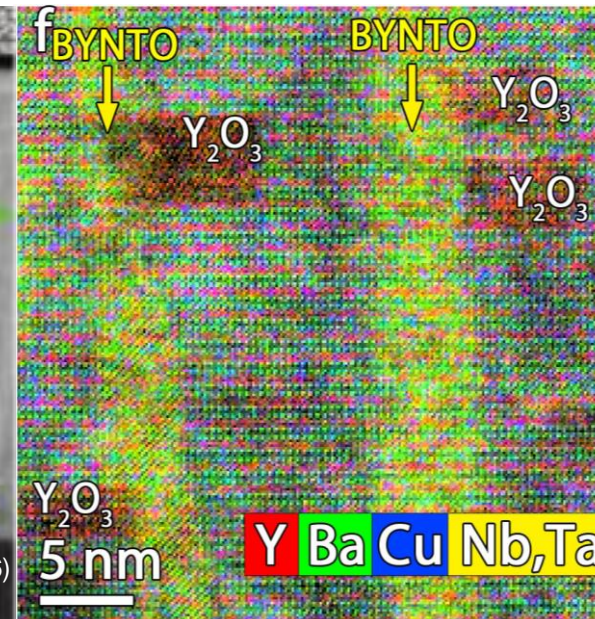
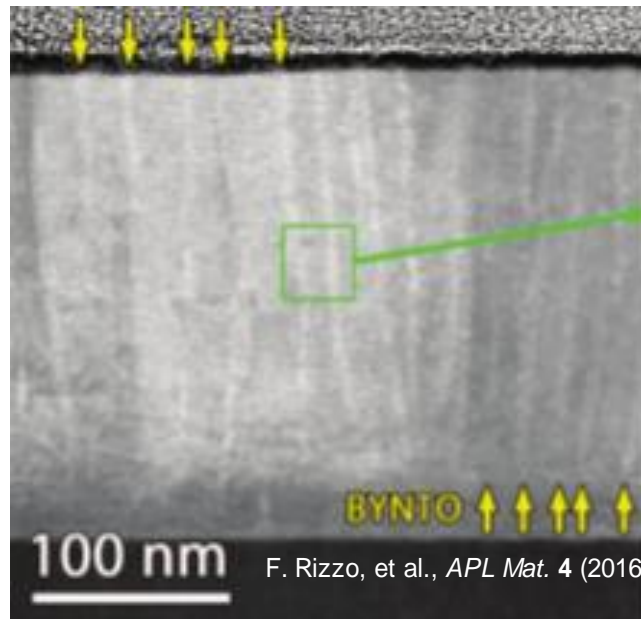
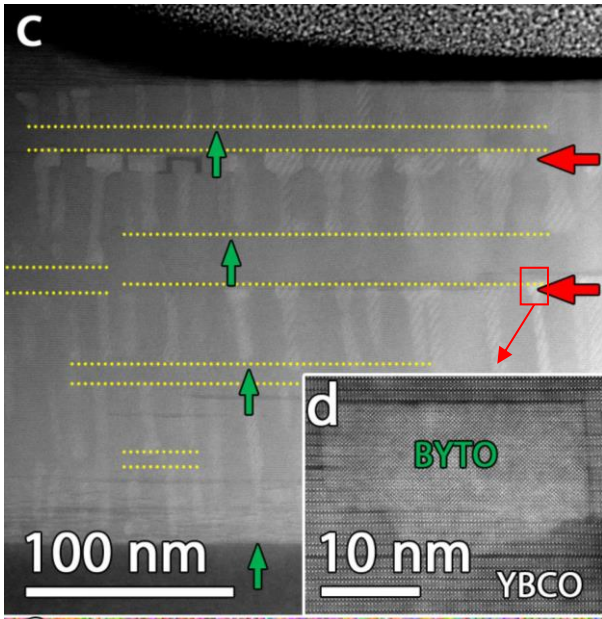
Mixed PLD nanocomposites BYNO +BYTO (BYNTO)

Combination of correlated defects along the c axis and ab-planes

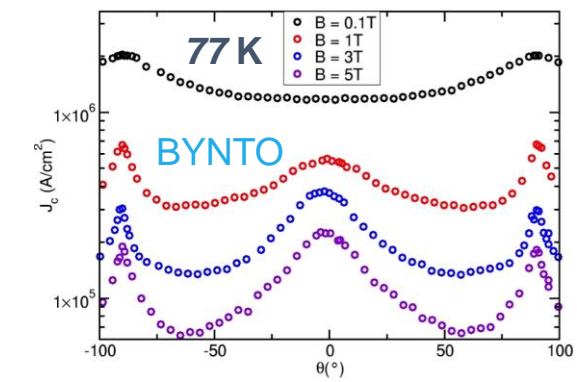
→ Complex and rich microstructure and capacity to tune the $J_c(\theta, H, T)$ dependence

Single (BYTO 5%) and mixed doping (BYNTO 5%) of YBCO on STO

Dense and fine columnar structure ($d \sim 5$ nm)



Continuous nanorods
Correlated pinning H//c

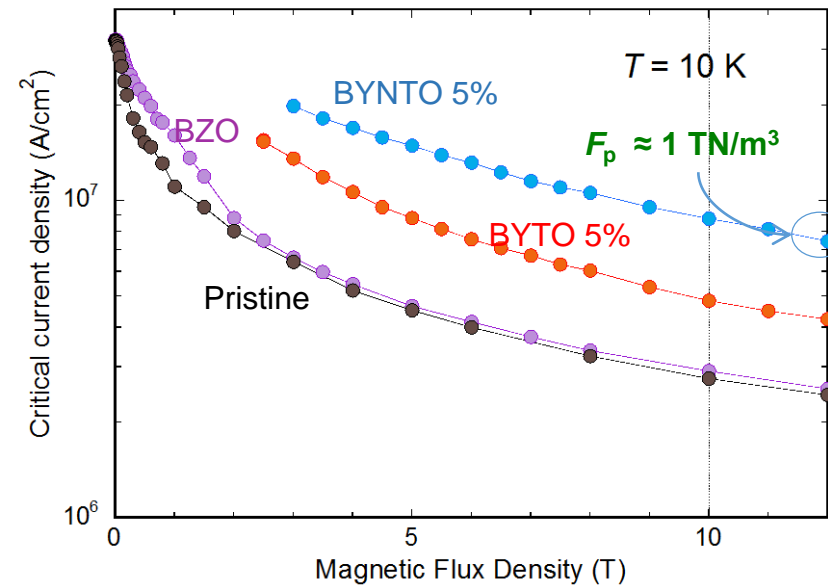
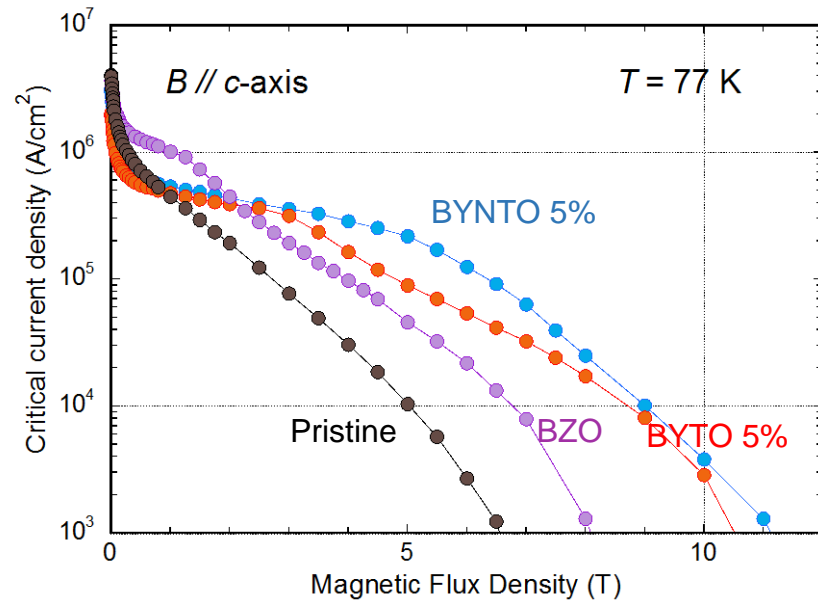


■ straight and partially interrupted columns in BYTO

■ splayed and continuous nanocolumns in mixed BYNTO

F. Rizzo, et al., submitted

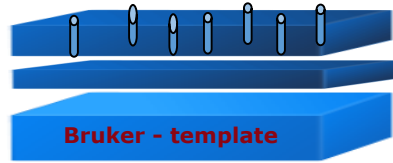
J_c properties BZO – BYTO - BYNTO APC



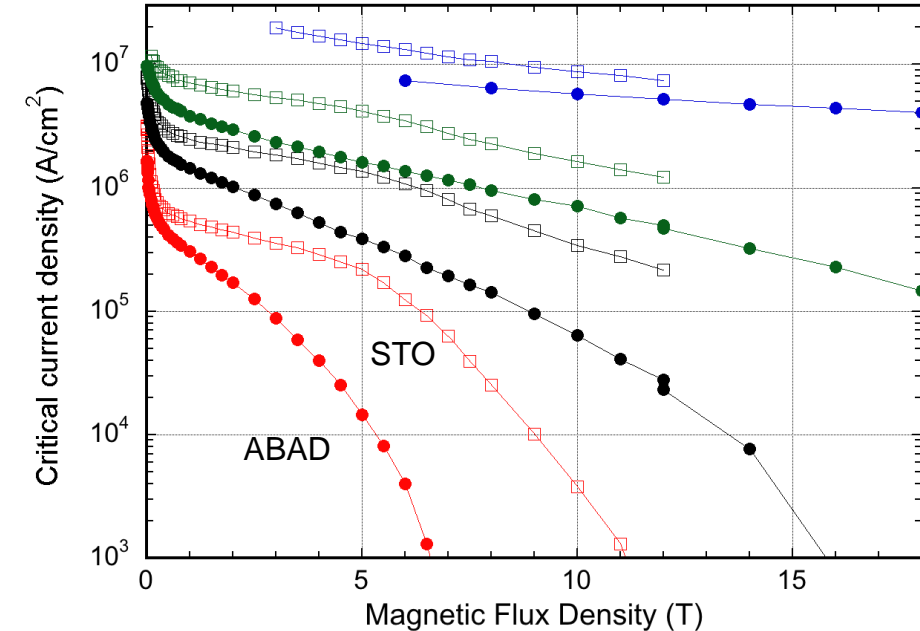
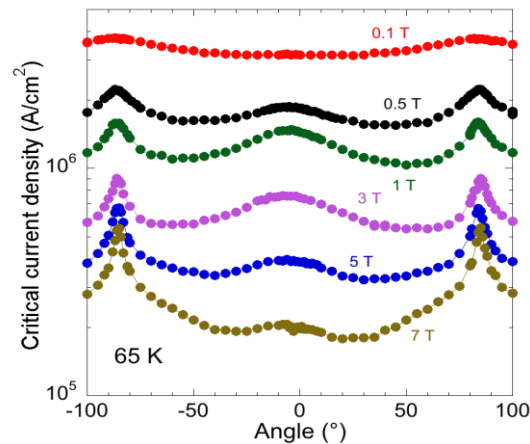
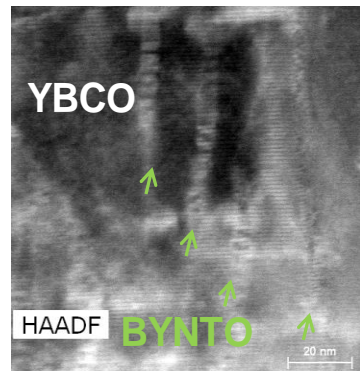
LN2 T range;

- BZO effective at low field
- BYNTO and BYTO at higher fields \Rightarrow Among highest values of B_{irr} (BYNTO) = 11 T for H//c
- BYNTO (mixed doping) more effective in both high field and low T regimes

YBCO + BYNTO on metallic ABAD CeO₂/YSZ/SS

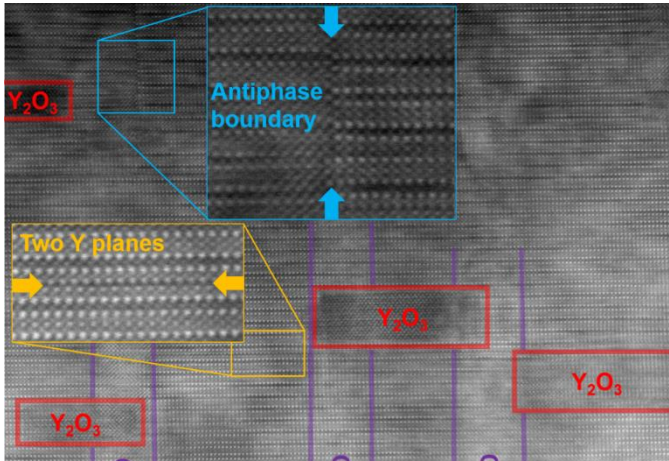


Multi-layers approach to avoid reactivity with the CeO₂ layer
 YBCO-BYNTO (150 – 250 nm) / YBCO (10-60nm) / ABAD



- higher T_c : similar to STO (≈ 88 K);
- Good J_c performances: closer to STO at lower T (to be still optimized)
- Formation of pinning effective BYNTO self assembled columns (to be still optimized, work is ongoing)

Density and morphology of defects can be tuned with f_{Dep}



- Very narrow BYNTO segmented nanocolumns
- Y_2O_3 plates
- Antiphase boundaries
- Stacking faults
- Dislocations

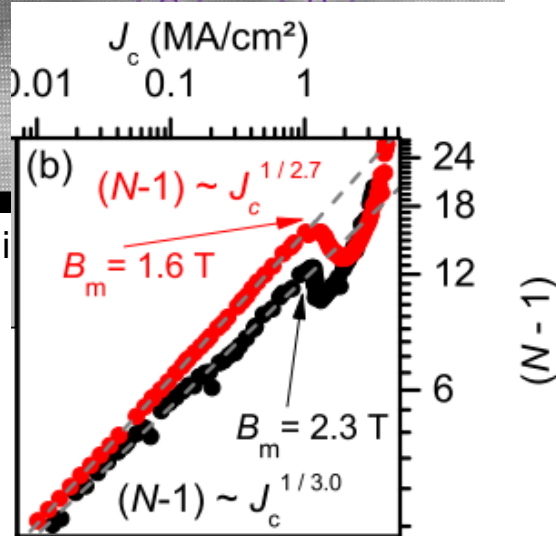
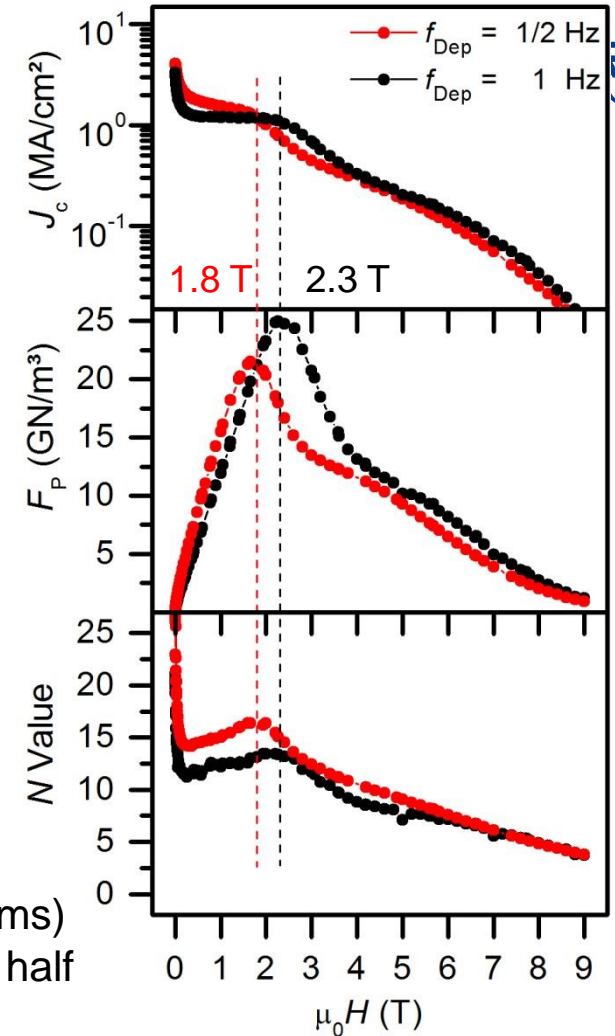
Increasing $f_{Dep} \Rightarrow$ Density of the nanorods \uparrow
 Diameter \downarrow
 Density of Y_2O_3 plates \uparrow

Matching effect for $B||c$

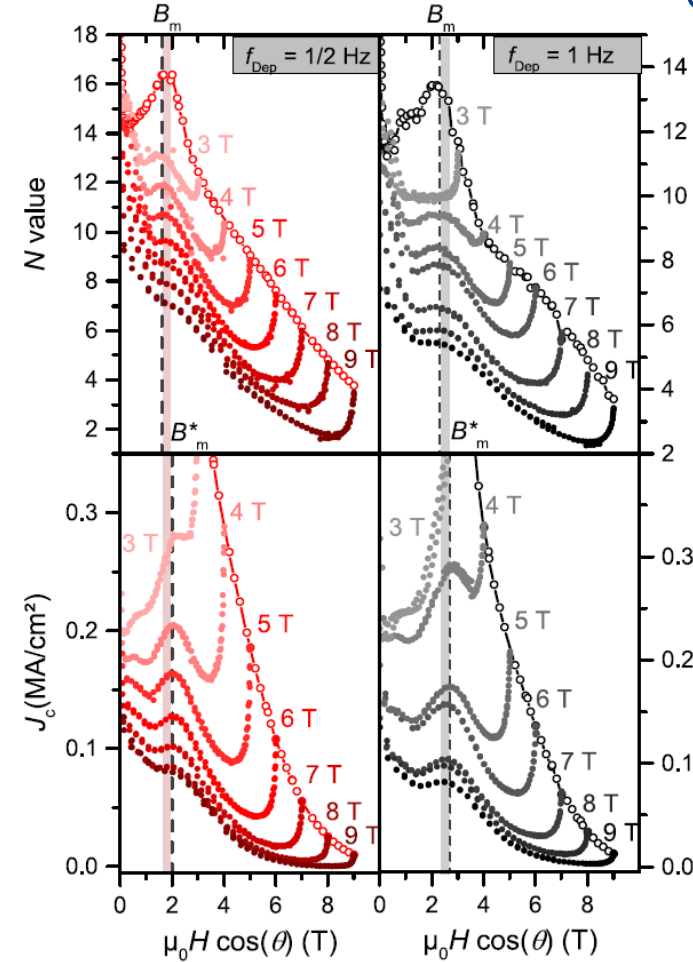
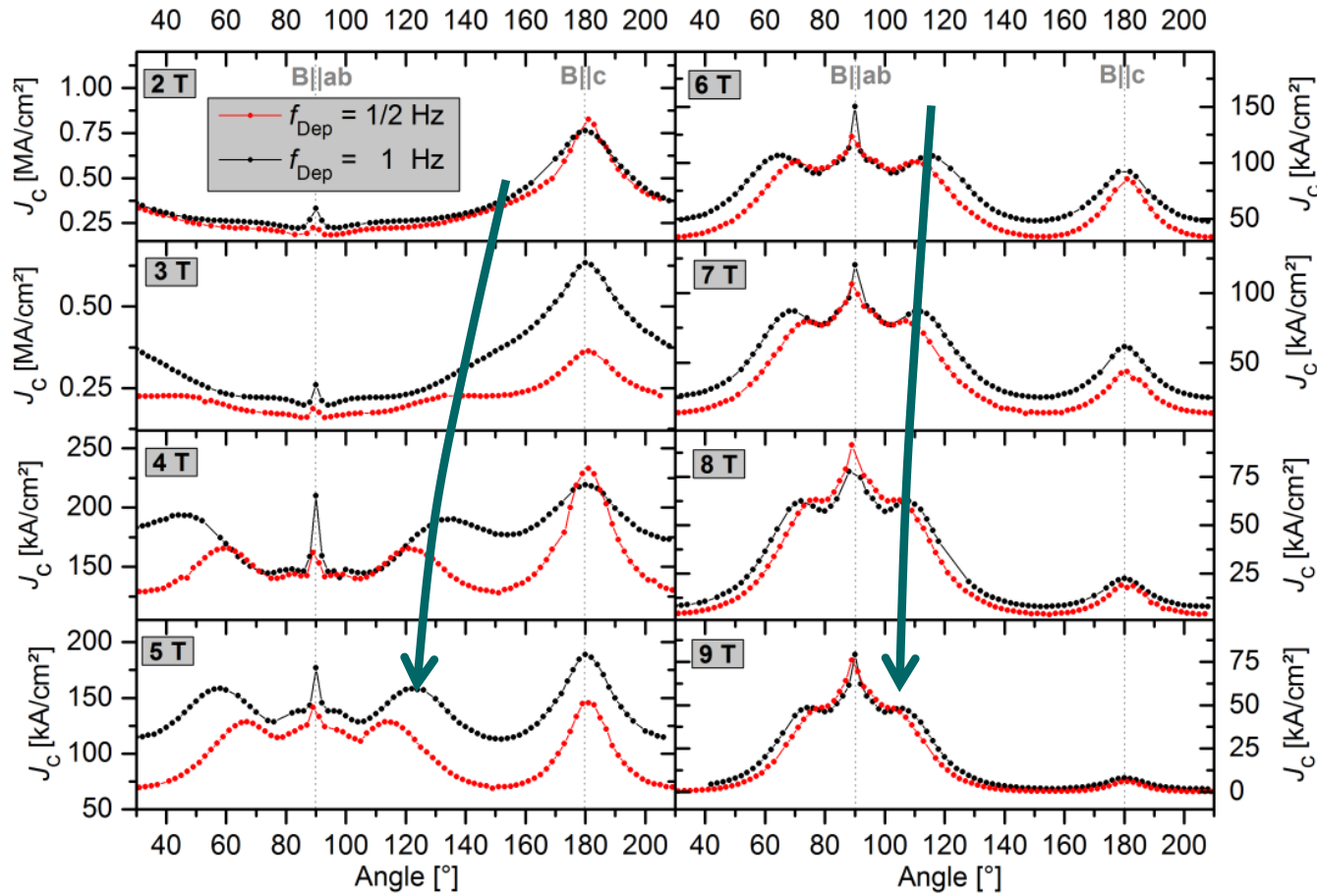
- End of J_c plateau
- F_p maximum (T independent)
- Peak in N value

High F_{pmax} (25 GN/m^3)
 among the highest values in literature!

- Anticorrelation $N - J_c$ below the matching field (nanocolumns)
- High $J_c \rightarrow$ Intermediate Y_2O_3 particles and SF hinder the half loops and double kink structures



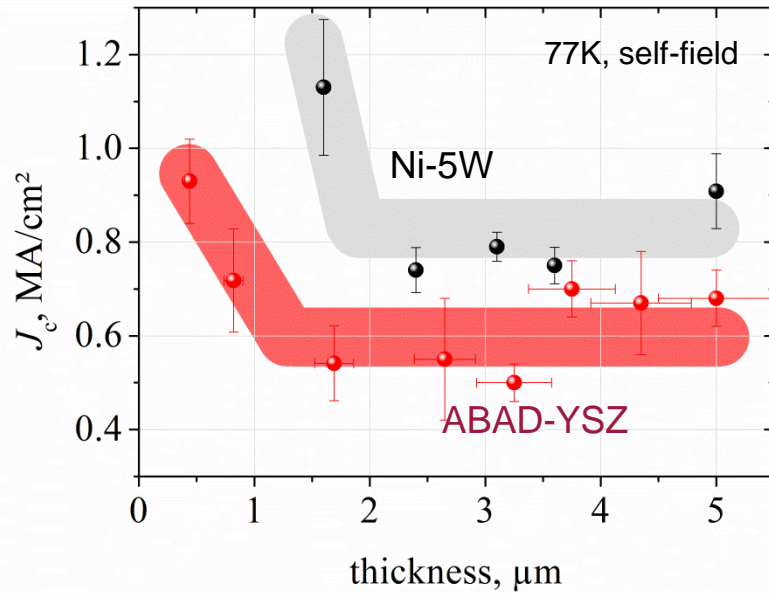
$t \sim 250 \text{ nm}$ thin



Complex J_c anisotropy (off axis peaks shifting towards the ab peak)

- Matching effect with c-axis component of applied field
- Region of N- J_c anticorrelation above the matching field

YBCO + 5 - 6 mol% BaHfO₃ (BHO)



5 μm thick BHO-doped YBCO layers:

$I_c \sim 350$ A/cm-width on ABAD-YSZ

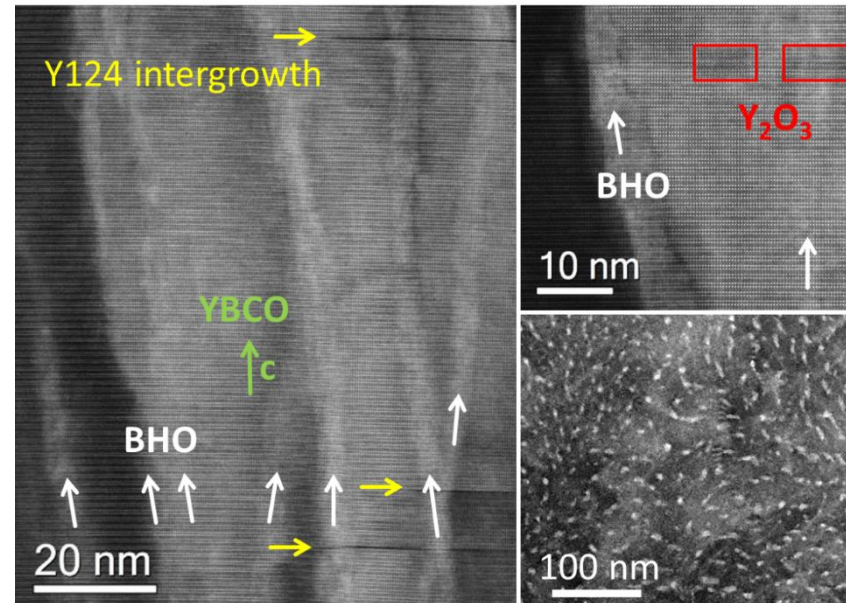
$I_c \sim 450$ A/cm-width on Ni-5W



Stainless steel / ABAD-YSZ / PLD-CeO₂
RABiT Ni-5 at.% W / CSD-La₂Zr₂O₇ / CSD-CeO₂



Influence of the Substrate

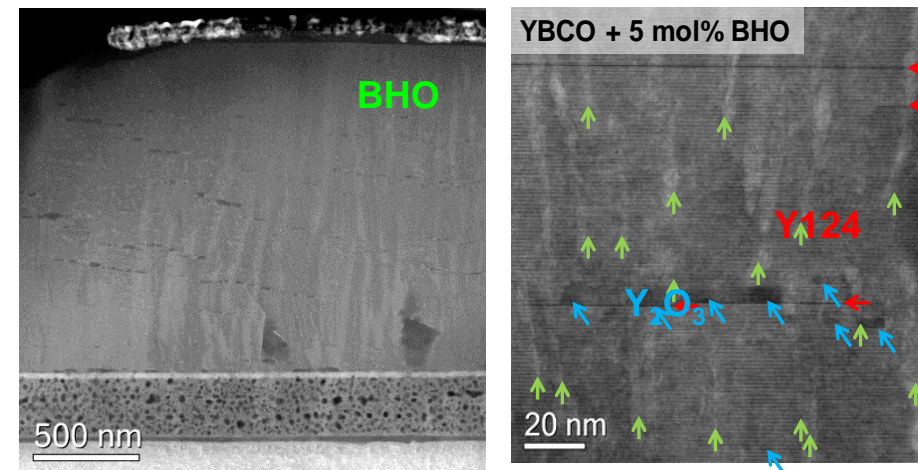


$R = 0.7$ nm/s

BHO-YBCO on ABAD-YSZ

→ Different defect landscape depending on the substrate used

- Fan-shaped BHO nanorods with diameter of (4 ± 2) nm and large splay (up to 20°)
- Y₂O₃ plates
- Y124 intergrowths

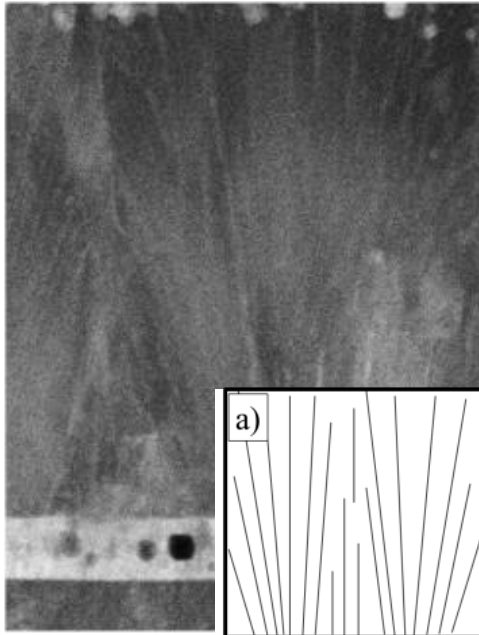


BHO-YBCO on Ni-5W

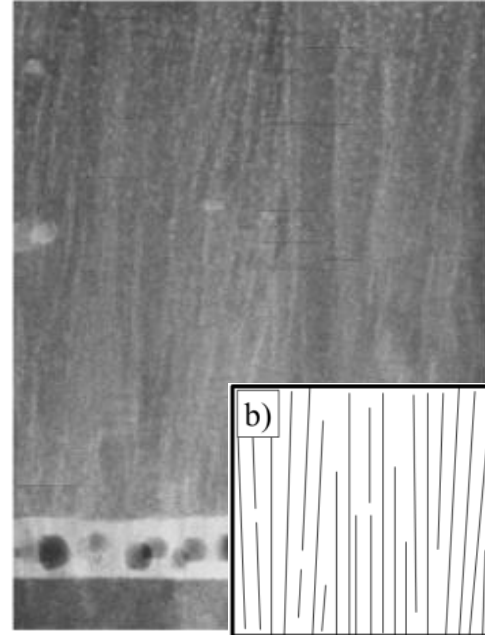


Influence of the growth rate

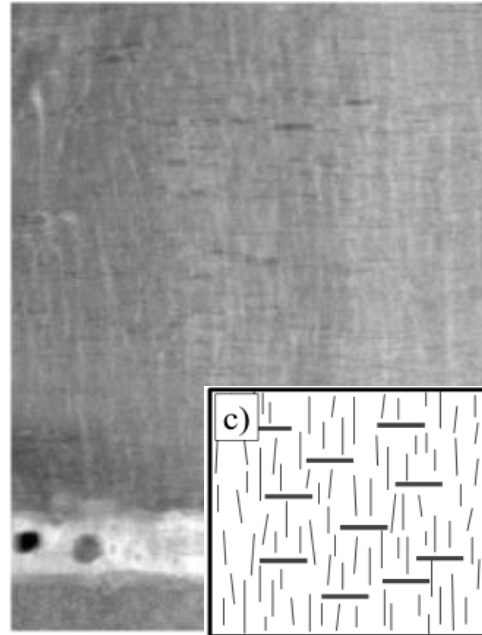
a) $R=0.4$ nm/s



b) $R=0.7$ nm/s

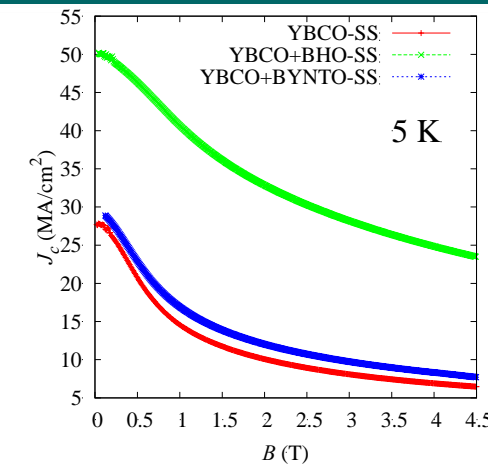
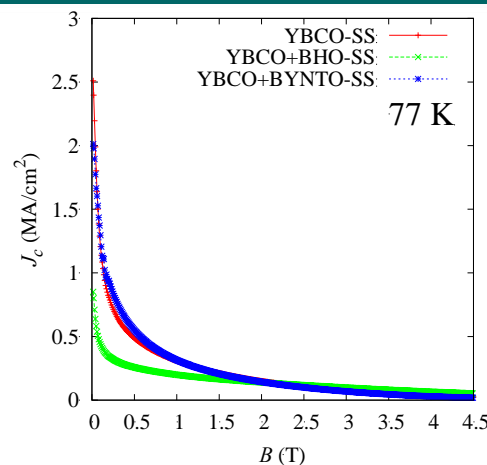
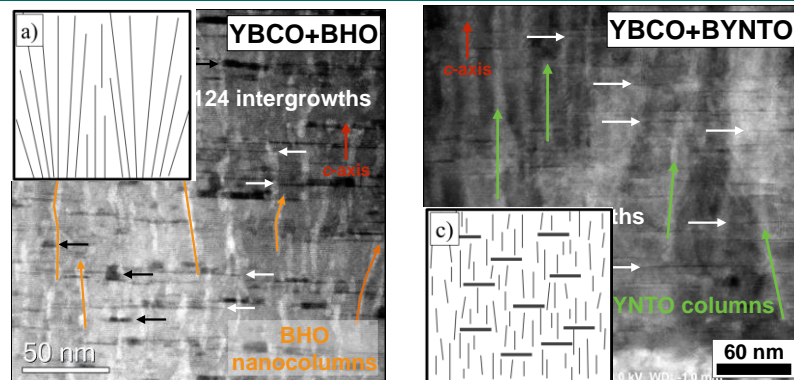


c) $R=1.2$ nm/s



- Growth rate 0.4 – 6.6 nm/s still epitaxial growth
- Changing distribution of pinning centers from **splayed nanorods** to mixture of **segmented nanorods** and **ab-oriented platelets**

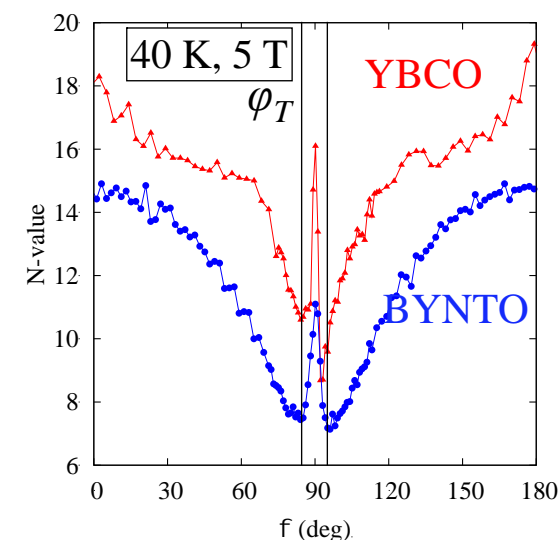
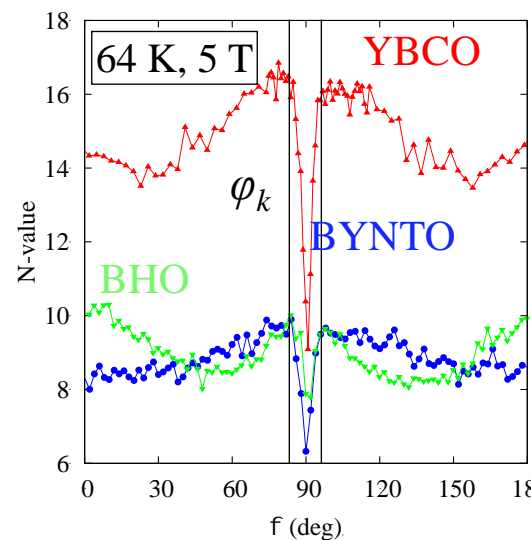
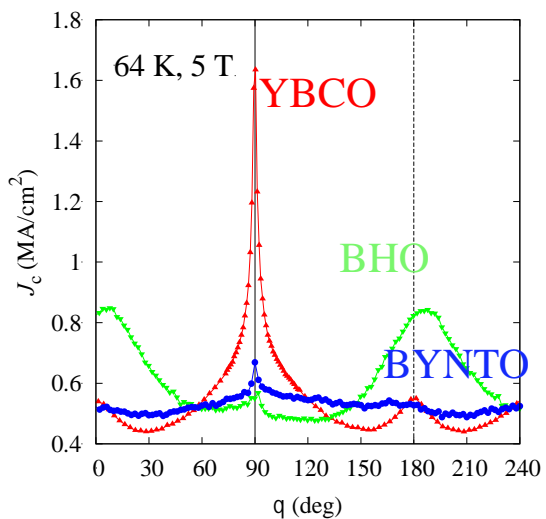
M. Sieger et al., IEEE Trans. Appl. Supercond. 27 (2017) 6601407



BHO show a larger J_c enhancement at low T

- Large splay nanorods
- Weak pinning??

Angular dependence



- Reduced peak for $B||ab$ due to defects
- Broad peak for $B||c$ for large splay of BHO nanocolumns
- Significantly reduced anisotropy for with mixed APC

- N lower in doped samples \rightarrow APC promote a higher creep rate
- Inverse $N(\theta) - J_c(\theta)$ correlation $H||ab$ (double kink excitations)
- **quasi-locked in state** manifested at 40 K as thermal activation is diminished

REBCO NANOCOMPOSITES GROWN BY CSD

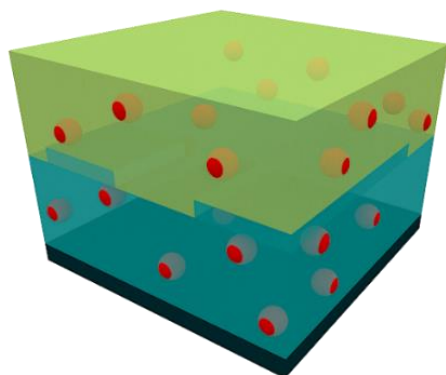
Sequential deposition and growth method

BaZrO₃ (BZO), BaHfO₃ (BHO), Ba₂YTaO₆ (BYTO) Ba₂Y(Nb_{0.5}Ta_{0.5})O₆ (BYNTO) ...



ReBCO Precursor Solution

- Addition of metal-organic salts
Spontaneous Segregation
- Colloidal Solution:
Preformed Nanoparticles



- Sequential growth
- Precursor Solution (TFA, Low Fluorine, TLAG)
- Deposition technique (spin coating, dip coating, slot die coating, ink jet printing)
- Growth conditions (T, Heating rate, PO₂, PH₂O, Gas velocity , P_{total})

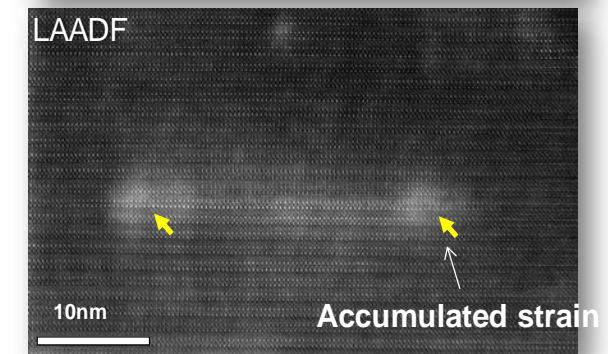
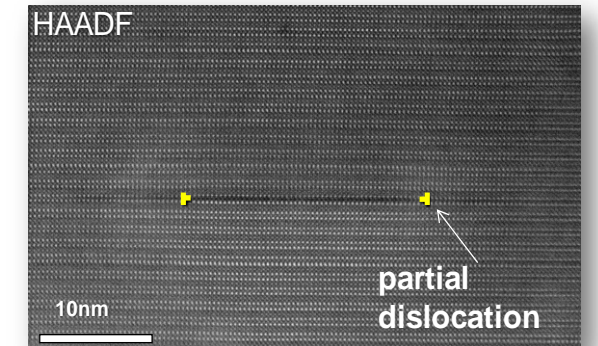
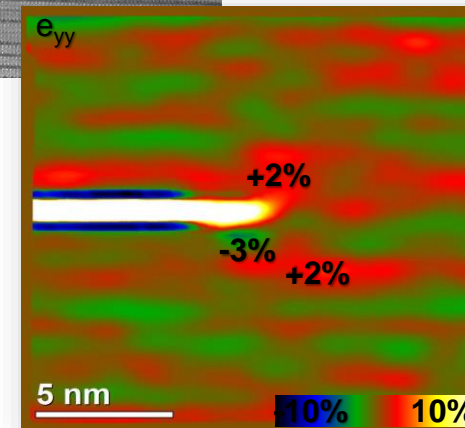
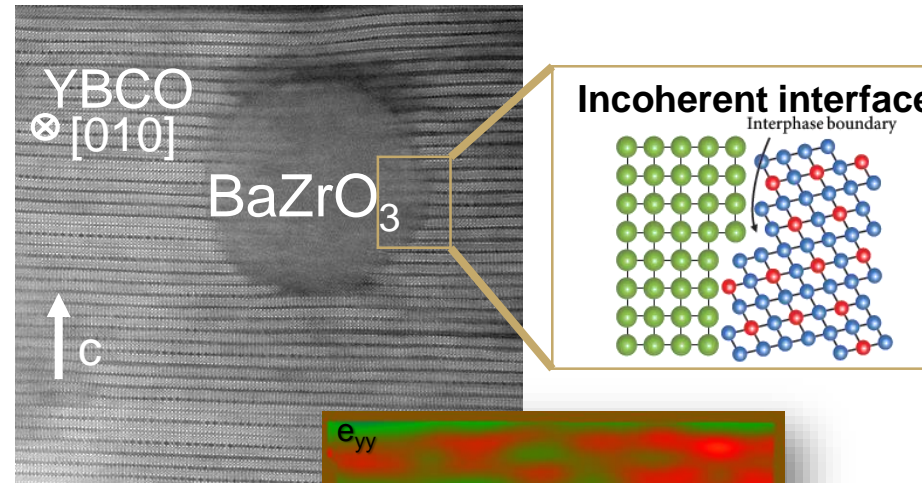
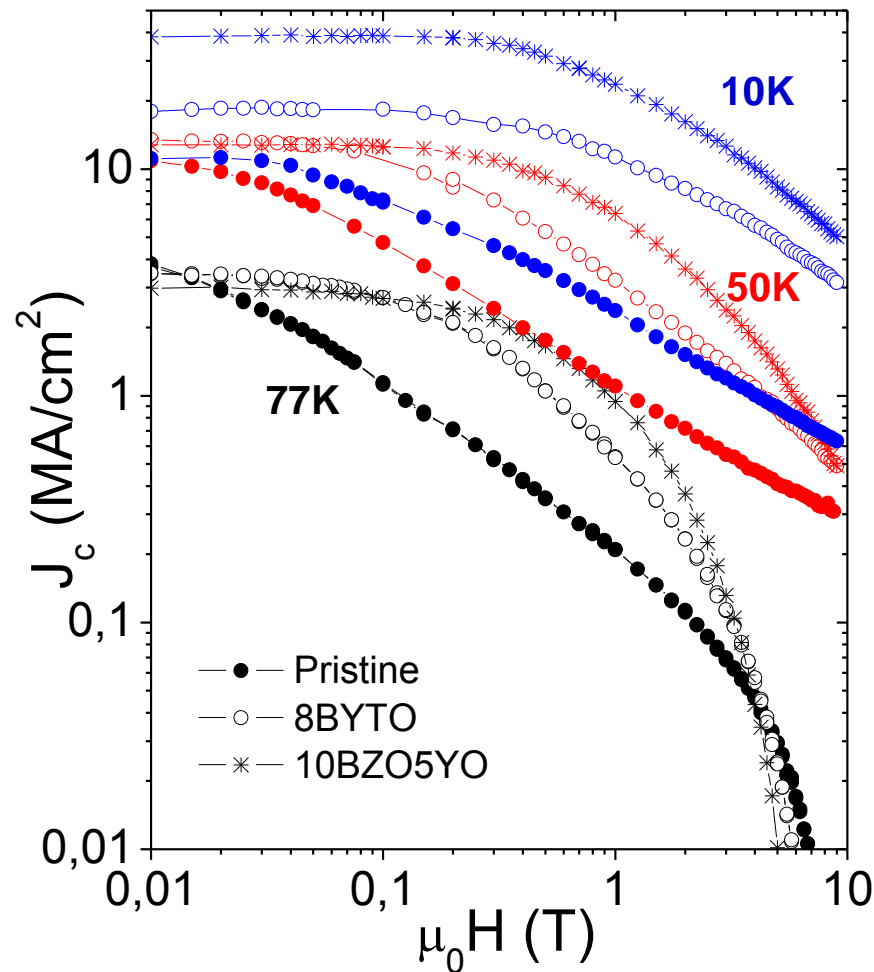
Vortex pinning mostly ascribed to distributed **local lattice distortions** (nanostrain) induced by defects generated due to the presence of nanoparticles

Self-assembled **randomly oriented** nanoparticles

HIGH PERFORMANCE OF CSD-YBCO NANOCOMPOSITES

CSD YBCO nanocomposites with different spontaneously segregated NP (BZO, BYTO, Y_2O_3 , ..)

Enhanced performance at all temperatures



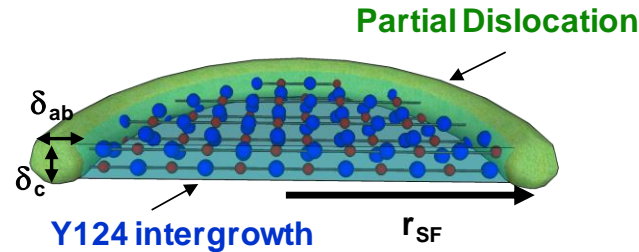
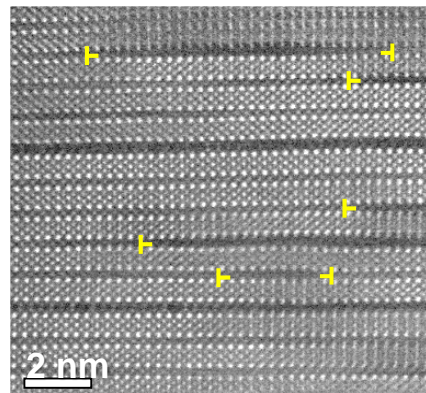
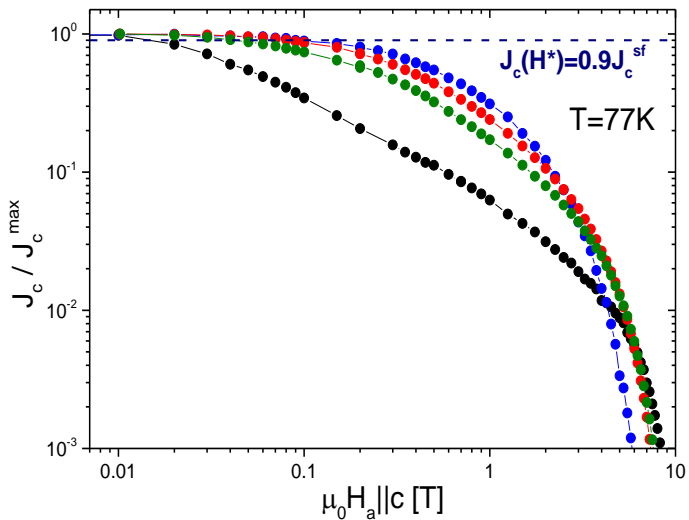
Strong strain effects are generated at the partial dislocations

Incoherent YBCO-NP interfaces give rise to **high density of Y248 intergrowths** (stacking faults) \Rightarrow Nanostrain associated to intergrowths

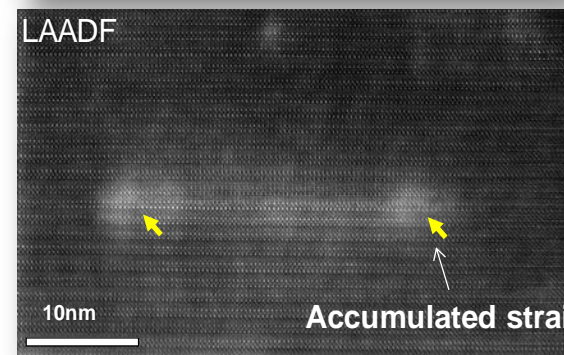
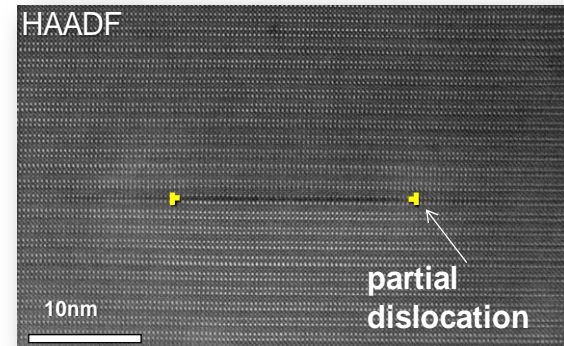
HIGH PERFORMANCE OF CSD-YBCO NANOCOMPOSITES

CSD YBCO nanocomposites with different spontaneous segregated NP (BZO, BYTO, Y₂O₃,..)

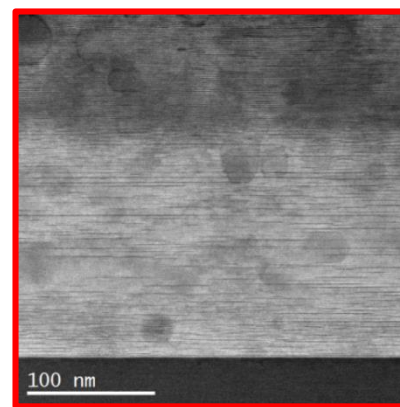
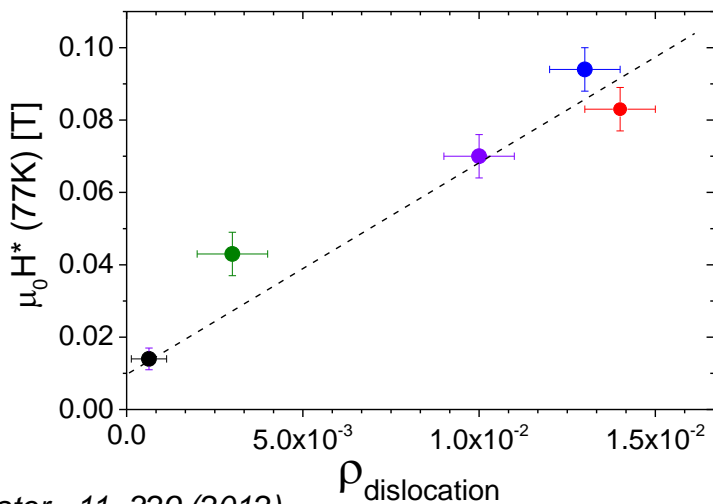
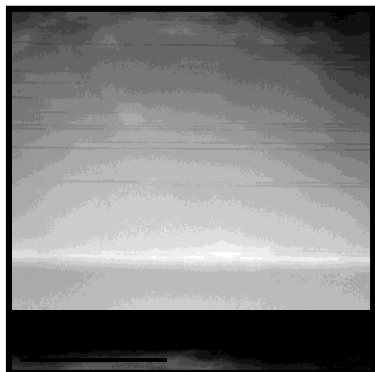
H*: single vortex pinning regime



$$\rho_{dislocation} = \frac{\pi \delta_c \delta_{ab}}{\Delta x \Delta y \langle r_{SF} \rangle} \left(n_{SF} \delta_{ab} + 2 \sum_{i=1}^{n_{SF}} r_{SF_i} \right)$$



Pristine

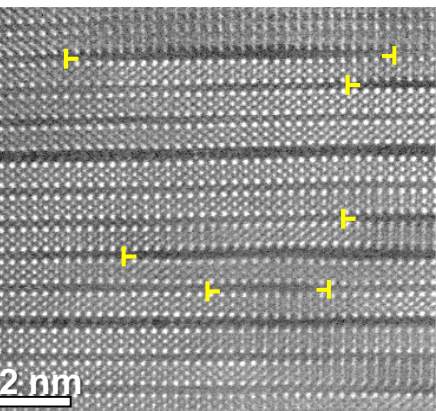
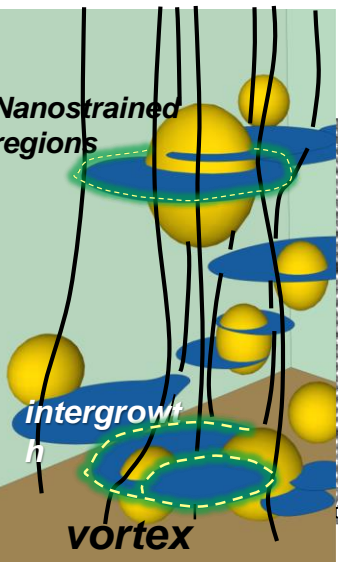
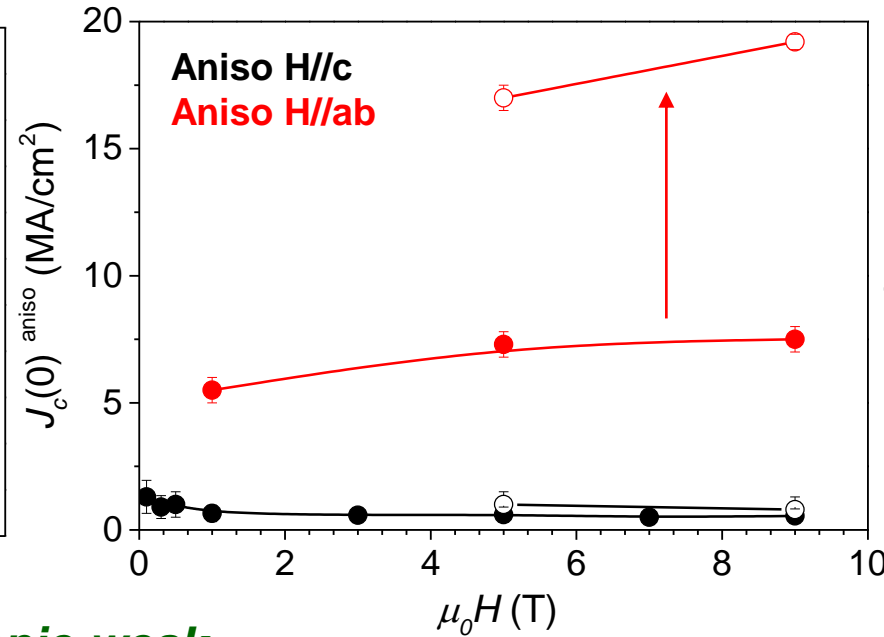
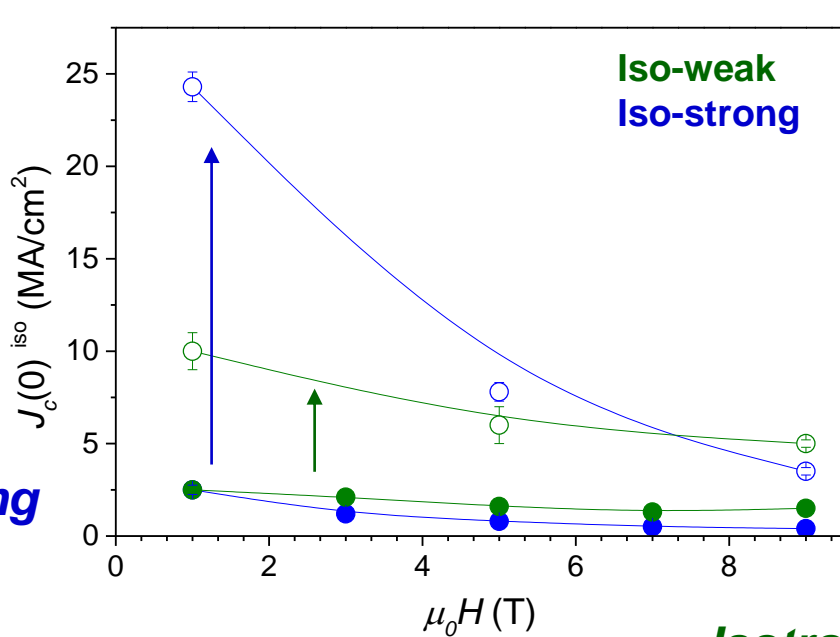


10% BZO/5% YO

Best route to obtain **high density of NP without segregation**

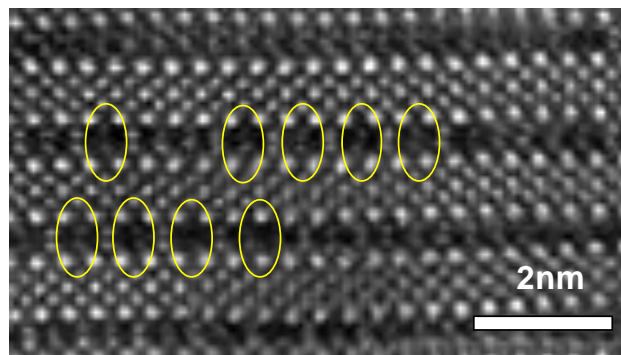
Mixed Nanocomposites (BZO/YO, BYTO/YO, BZO/BYTO) with optimized growing conditions → high density of short SF defect landscape

VORTEX PINNING CONTRIBUTIONS IN CSD NANOCOMPOSITES



strain induced

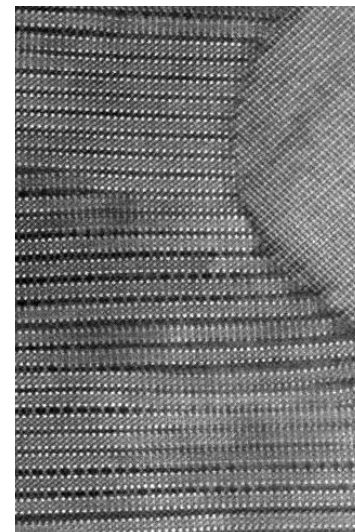
Isotropic-weak



Weak pinning contribution: Cu-O cation vacancies

New point defects effective at low temp.

Anisotropic H//ab

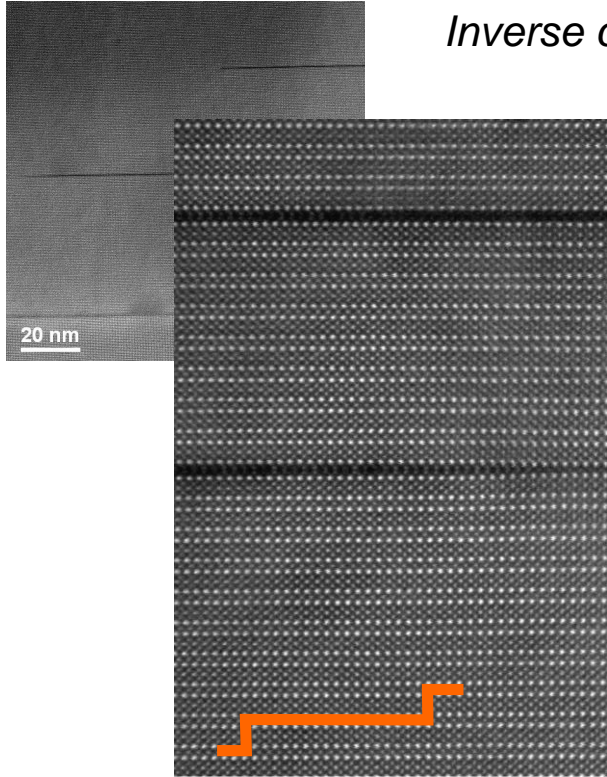


SF correlated defects along the a-b planes

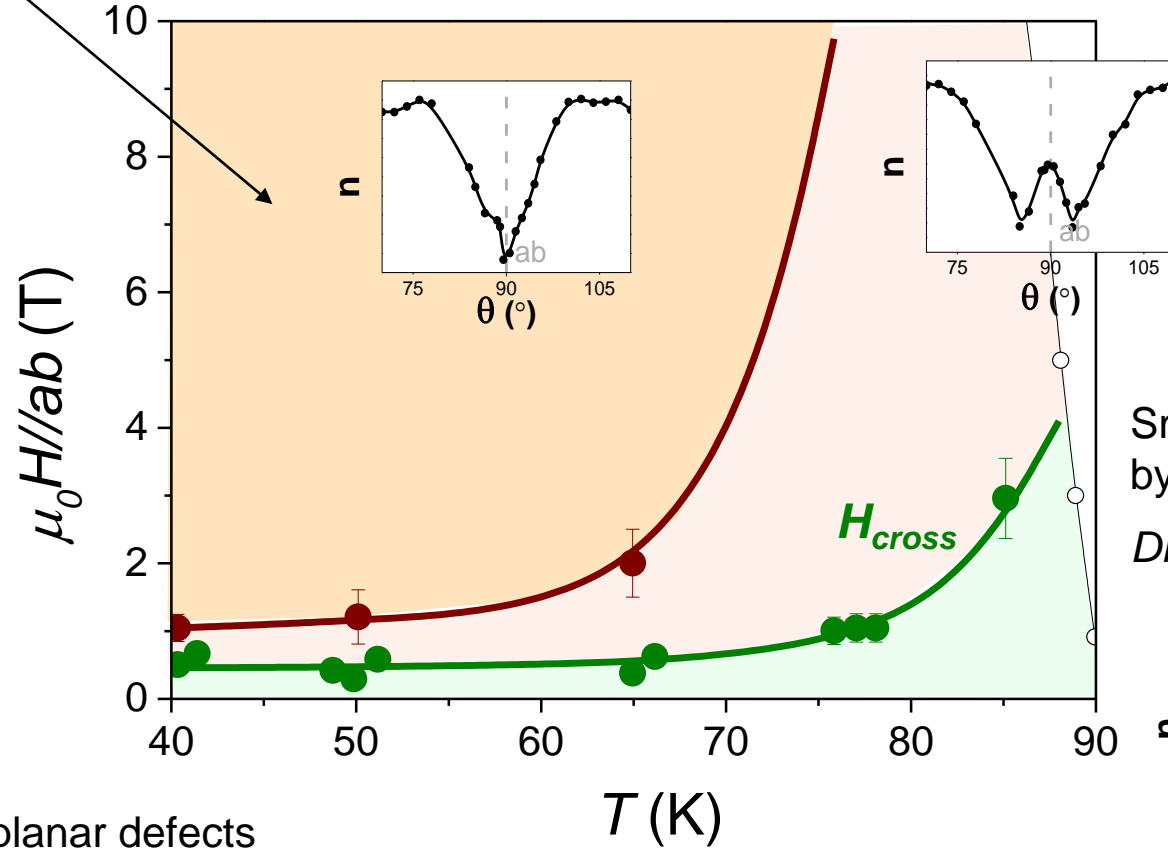
Staking Faults: multiple pinning sites of different dimensionality

STACKING FAULTS AVOID THE DOUBLE KINK FORMATION (H//ab)

Pristine YBCO



Inverse correlation J_c and N



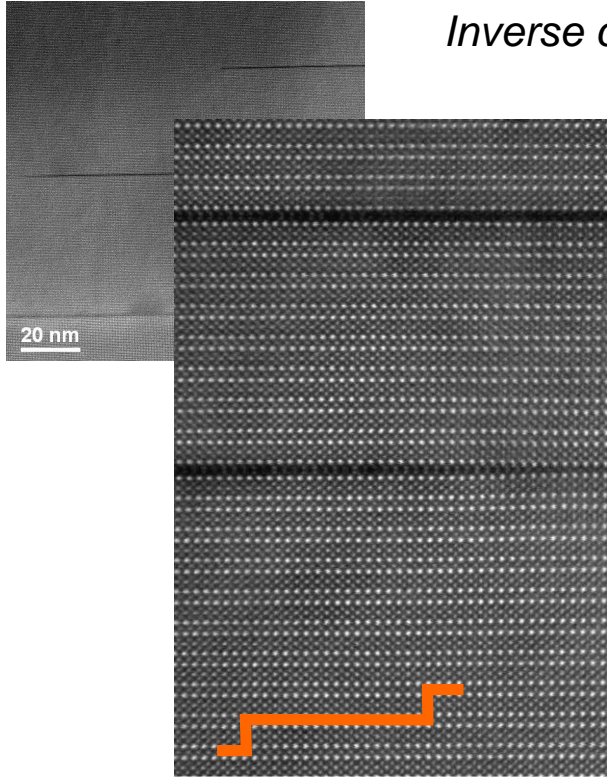
a-b planes → strongly correlated planar defects
 Large region dominated by Intrinsic pinning (double kink excitations)

Creep ↑↑

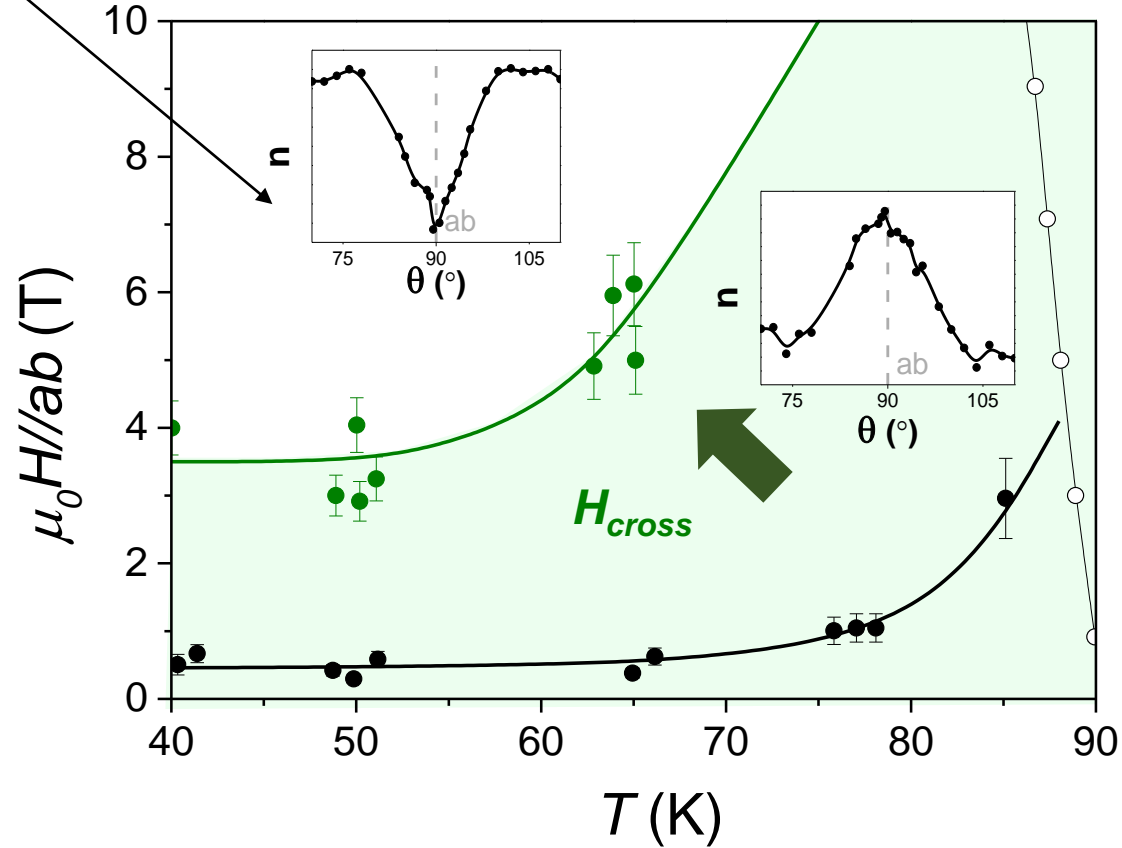
Creep ↓↓

STACKING FAULTS AVOID THE DOUBLE KINK FORMATION (H//ab)

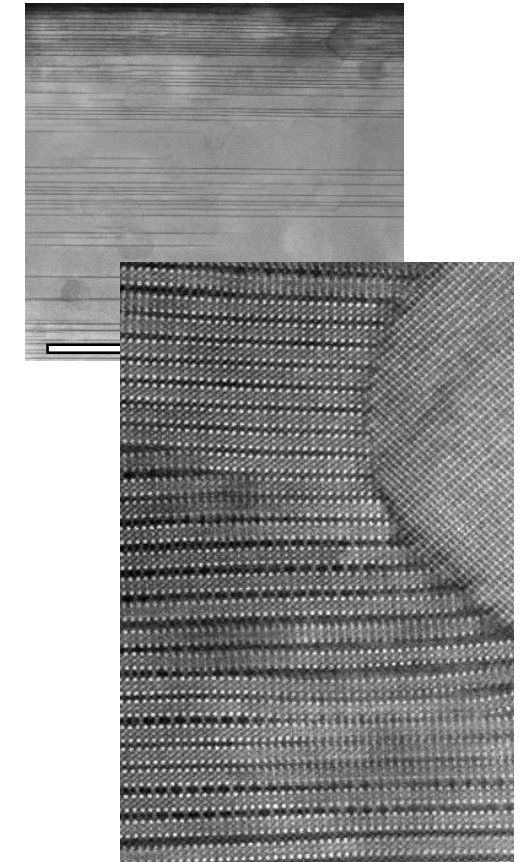
Pristine YBCO



Inverse correlation J_c and N



Nanocomposite



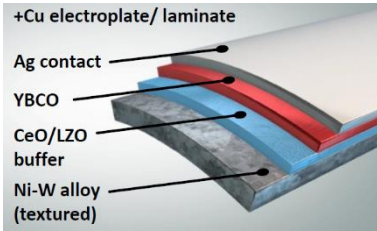
Nanocomposites → Strongly distorted matrix due to the presence of SF

The region dominated by SF pinning is enhanced to higher fields ⇒ **Reduce H - T region with double kink excitations**

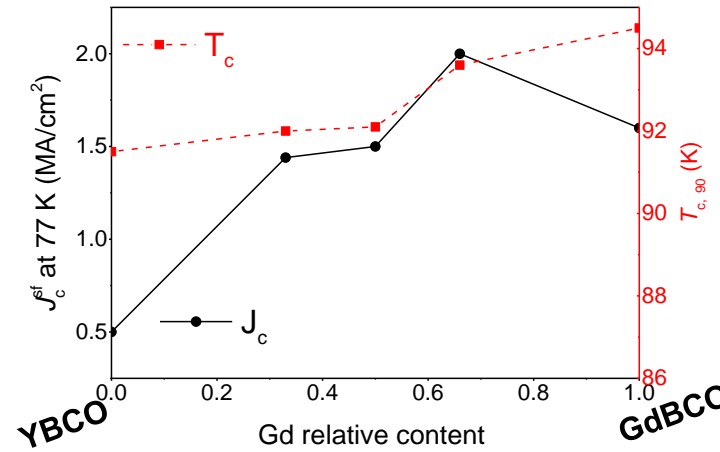
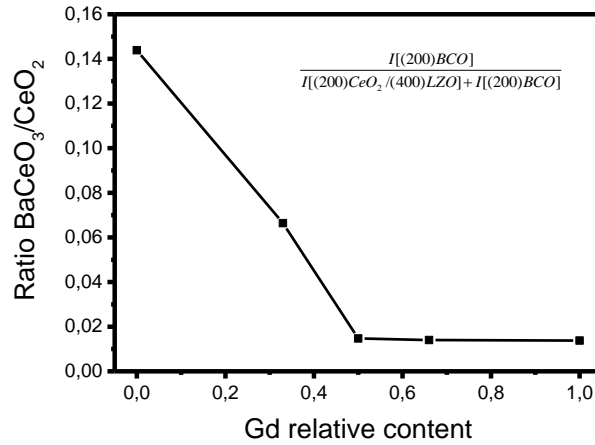
Creep ↓↓

CSD (Y,Gd)BCO+BHO FILMS ON RABBIT TAPES

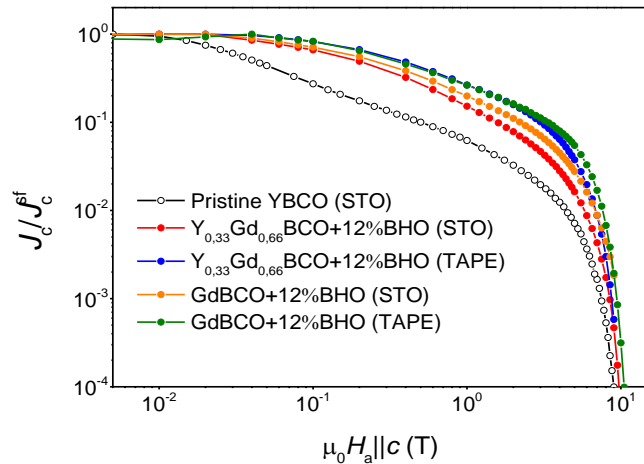
(Y,Gd)BCO+12%BHO films with different Y and Gd ratios.



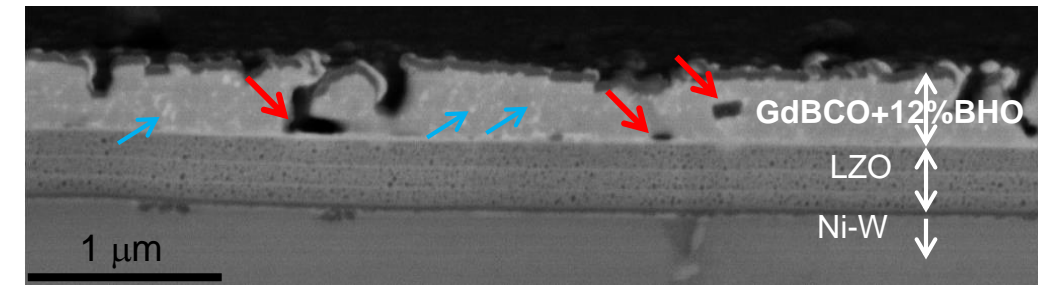
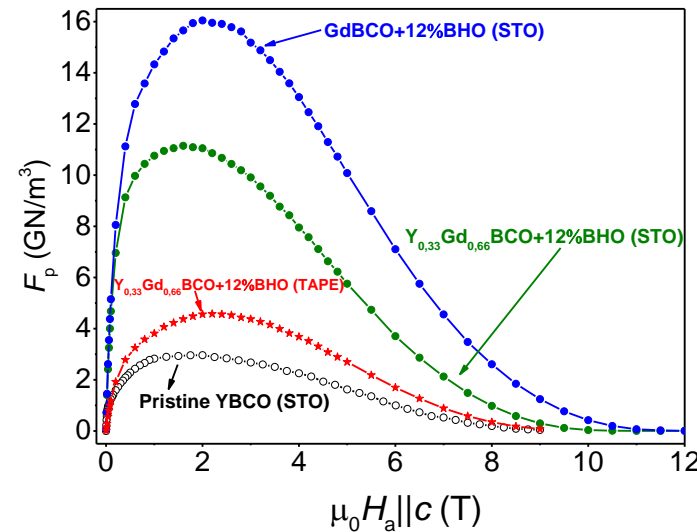
Ni-W /CSD LZO / CeO²
Growth temperature: 790 °C



- BaCeO₃ formation reduces as the Gd content increases
- J_c ~ 2 MA/cm² for 200 nm on tapes
- Similar T_c values than in STO.



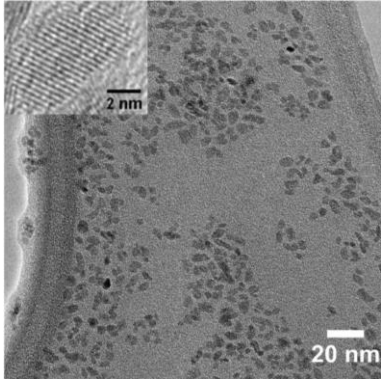
- smoother dependency (similar behaviour than SC)



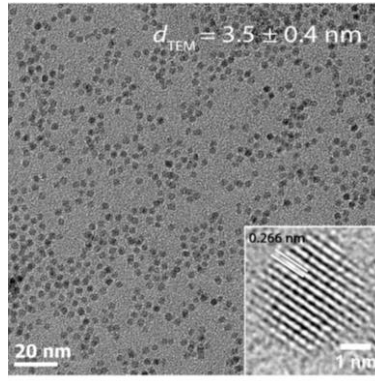
- GdBCO +12%BHO on SC ⇒ F_p ~ 16 GN/m³
- YGdBCO +12%BHO on tape ⇒ F_p ~ 5 GN/m³ (higher than the pristine sample on STO)
- Promizing results but still limited by pores in the matrix → further optimization is required

CSD WITH PREFORMED NANOCRYSTALS / NANOPARTICLES

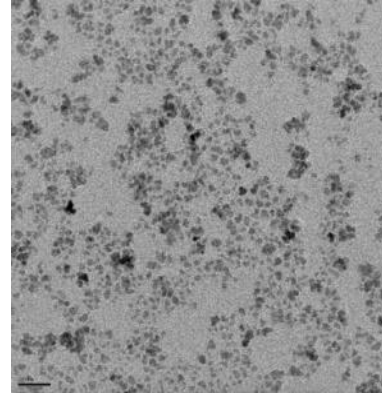
Monocl. ZrO₂ (10-12 nm)



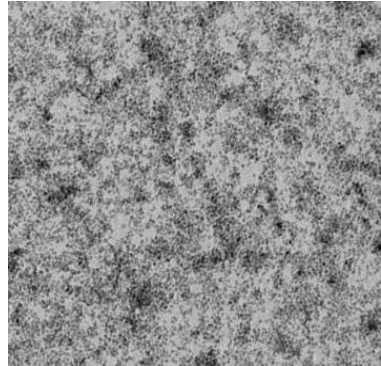
Cubic ZrO₂ (3-4 nm)



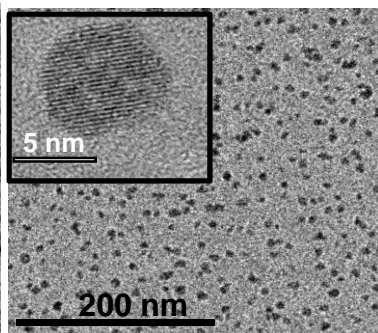
CoFe₂O₄ (5-6 nm)



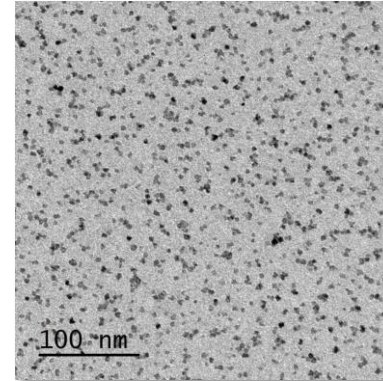
CeO₂ NPs (2-3 nm)



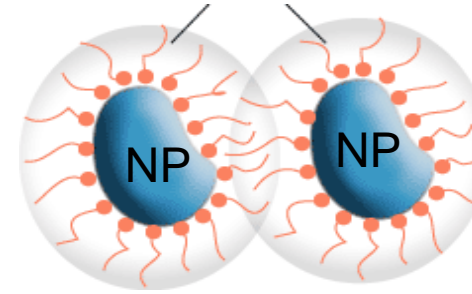
BaHfO₃ (5-8 nm)



BaZrO₃ (4-5 nm)



Stabilizing compound



Requirements:

- Small size (< 10 nm range)
- Narrow size dispersion
- High concentrations (~100 mM)
- Highly crystalline
- Highly dispersive
- Stable in alcoholic media
- Stable in YBCO ionic environment

Oxide nanoparticles can be stabilized in the YBCO precursor solution at high concentrations



Better control of size, density

New phases must be explored (magnetic NP)



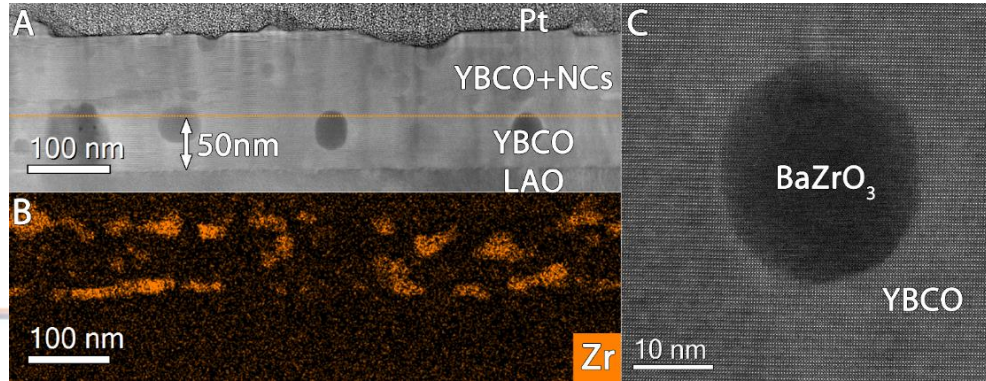
deutsche
nanoschicht



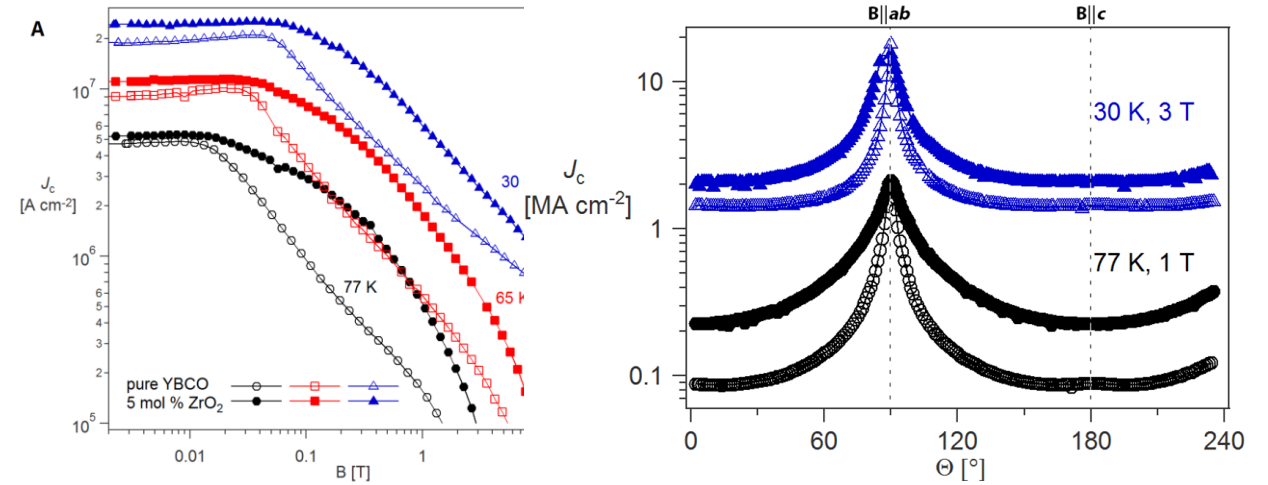
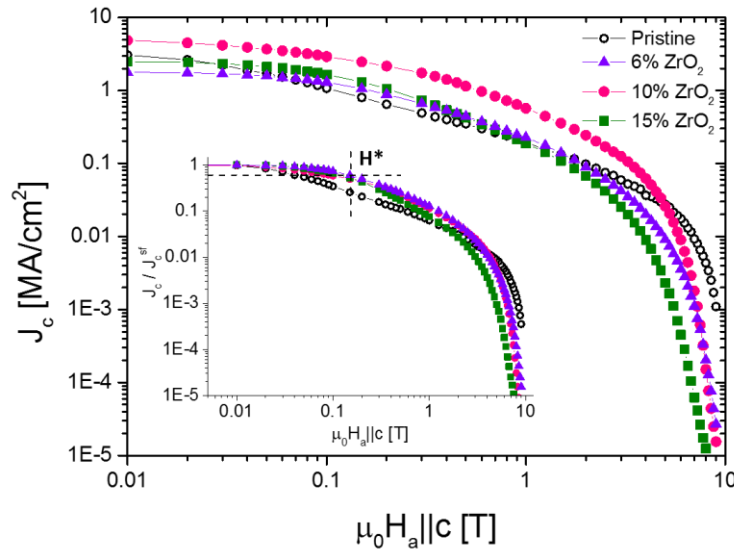
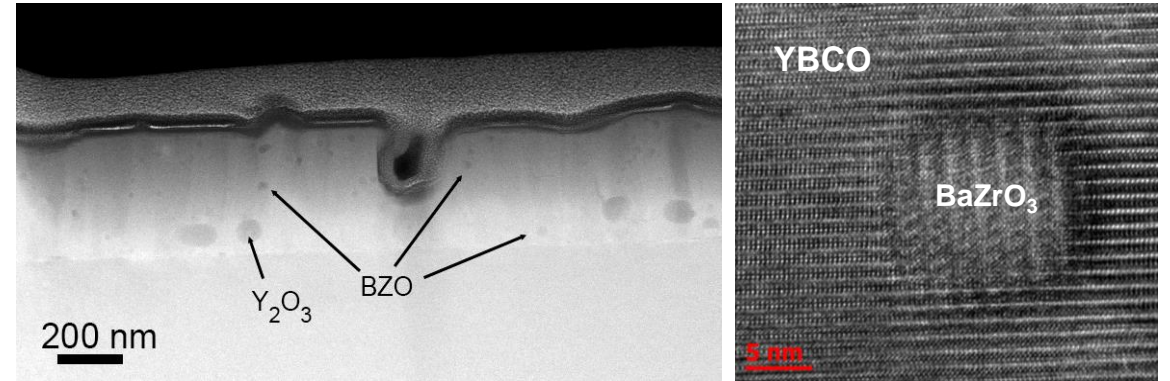
CSD YBCO Nanocomposites (ZrO₃ preformed NP)



TFA YBCO



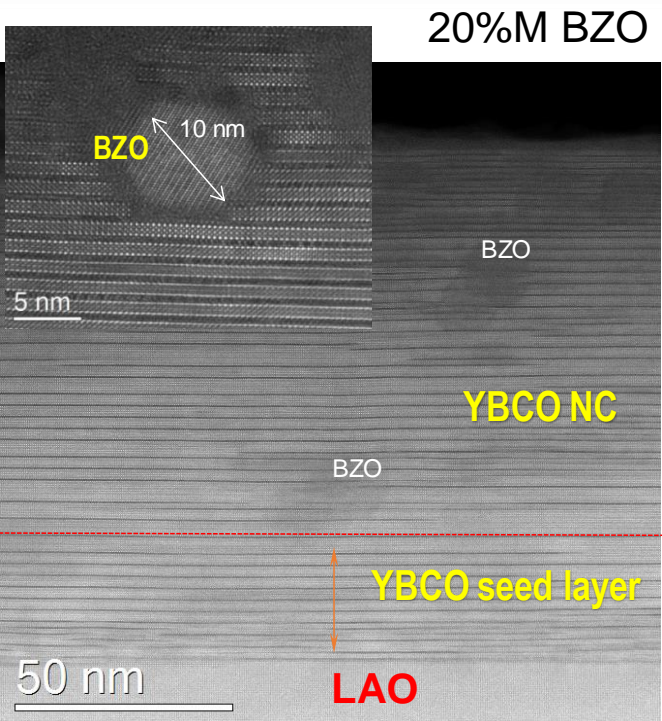
Low-fluorine YBCO



- Reactivity (BaZrO₃)
- NC with homogeneous dispersion of NC

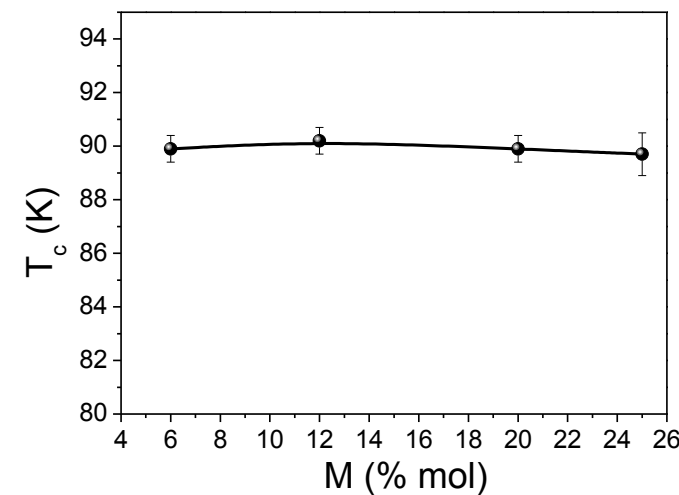
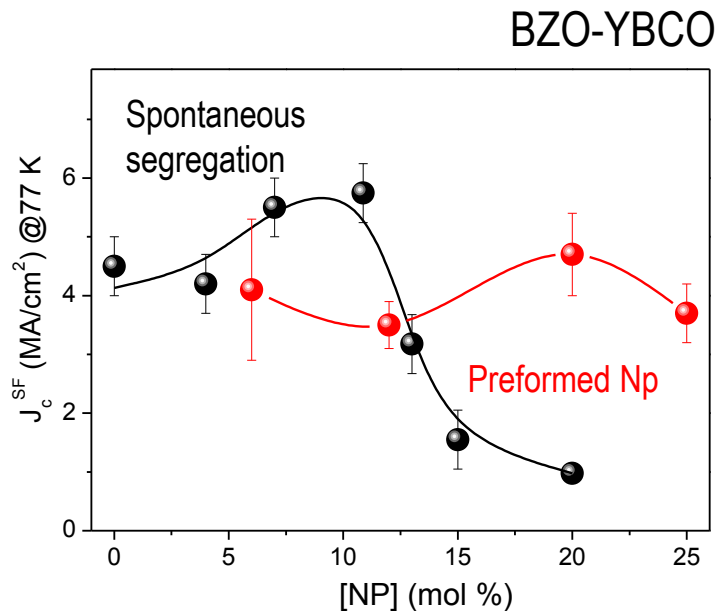
Improved J_c(H) performance

NON-REACTIVE PREFORMED BaZrO₃ and BaHfO₃ NANOPARTICLES

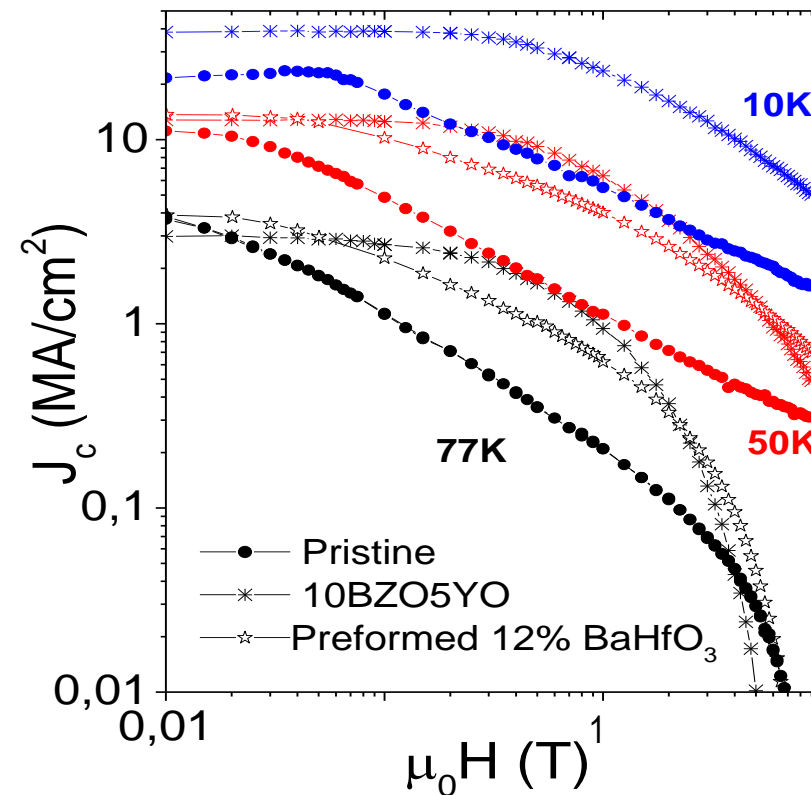


20%M BZO

- No reactivity nor coarsening occurs
- High homogeneity in Np dispersion



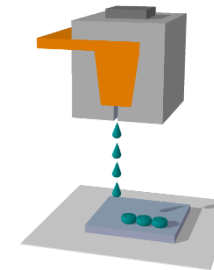
- Higher concentration of Np without current blocking
- No T_c reduction up to 25 %



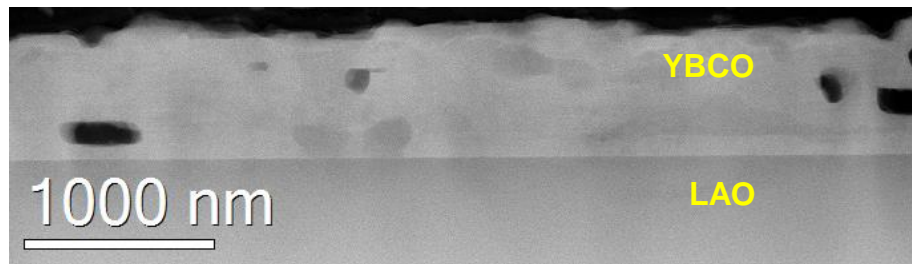
- J_c (sf) = 3-5 MA/cm² at 77 K, 200 nm
- High performance at all temperatures

THICK NANOCOMPOSITES WITH PREFORMED NANOPARTICLES

- Colloidal solutions compatible with IJP
- Thick layer and CC are reachable

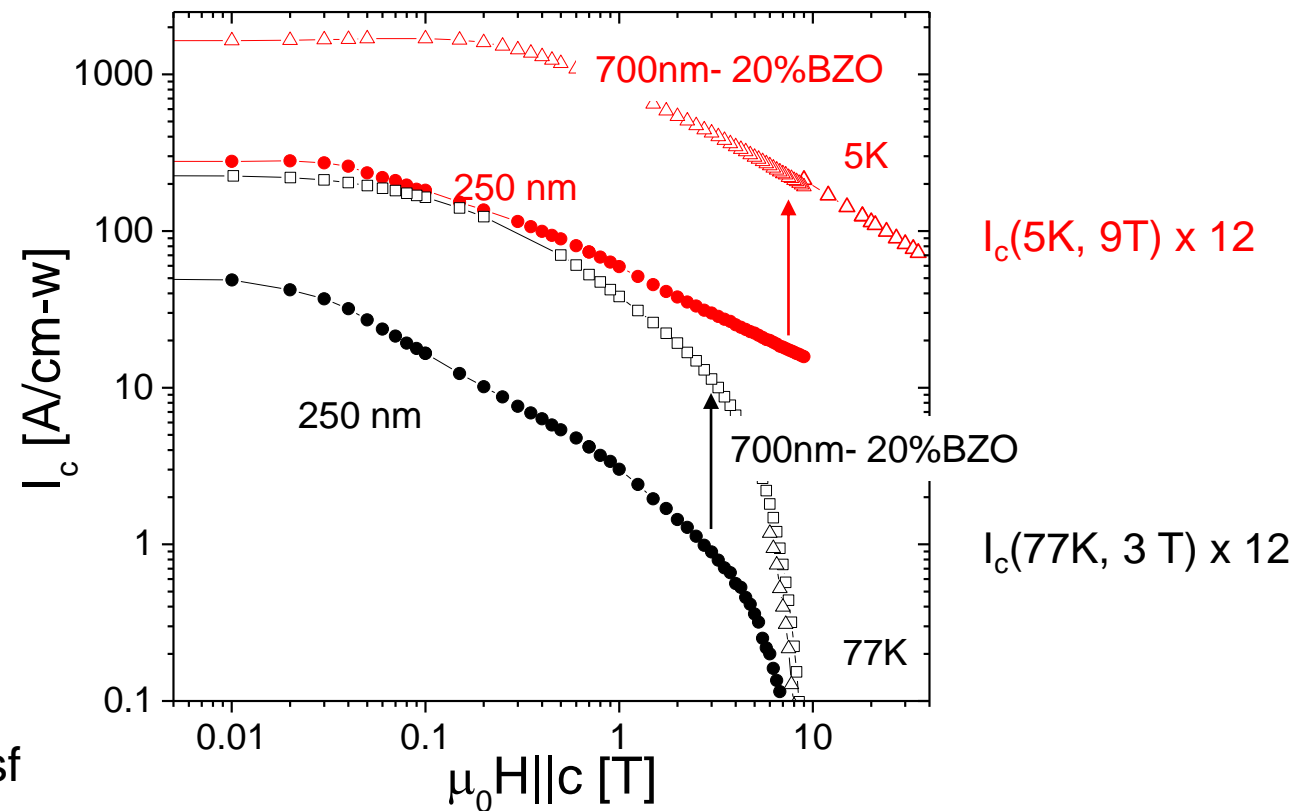
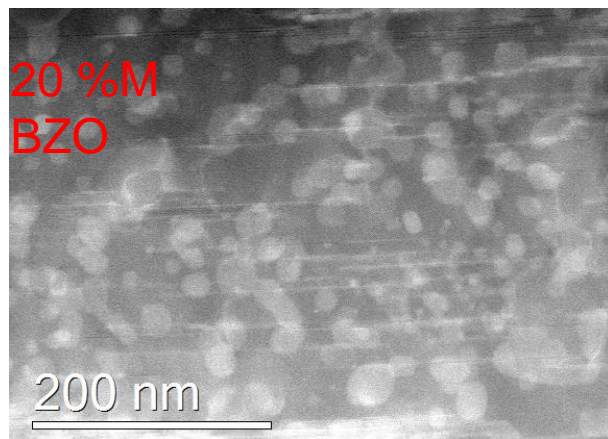


IJP single deposition



Increase of I_c with thickness by IJP deposition of nanocomposites

Well dispersed NP



700-850 nm single deposited BZO nanocomposites with $J_c = 3-3.5 \text{ MA/cm}^2$ at 77K, sf, $I_c \sim 240 \text{ A/cm-w}$ 77, sf

THICK NANOCOMPOSITES ON METALLIC SUBSTRATE



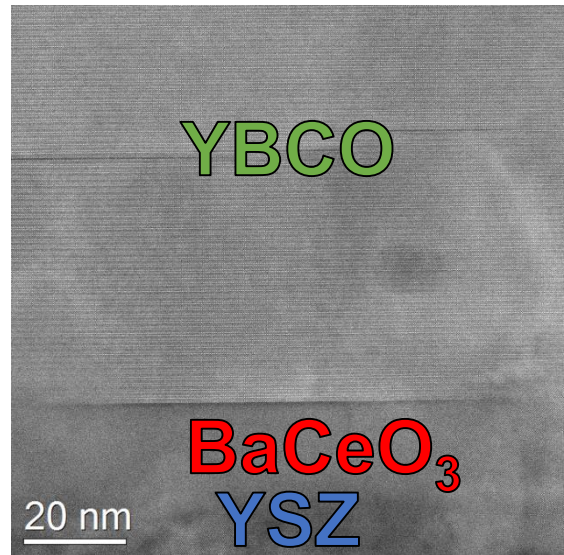
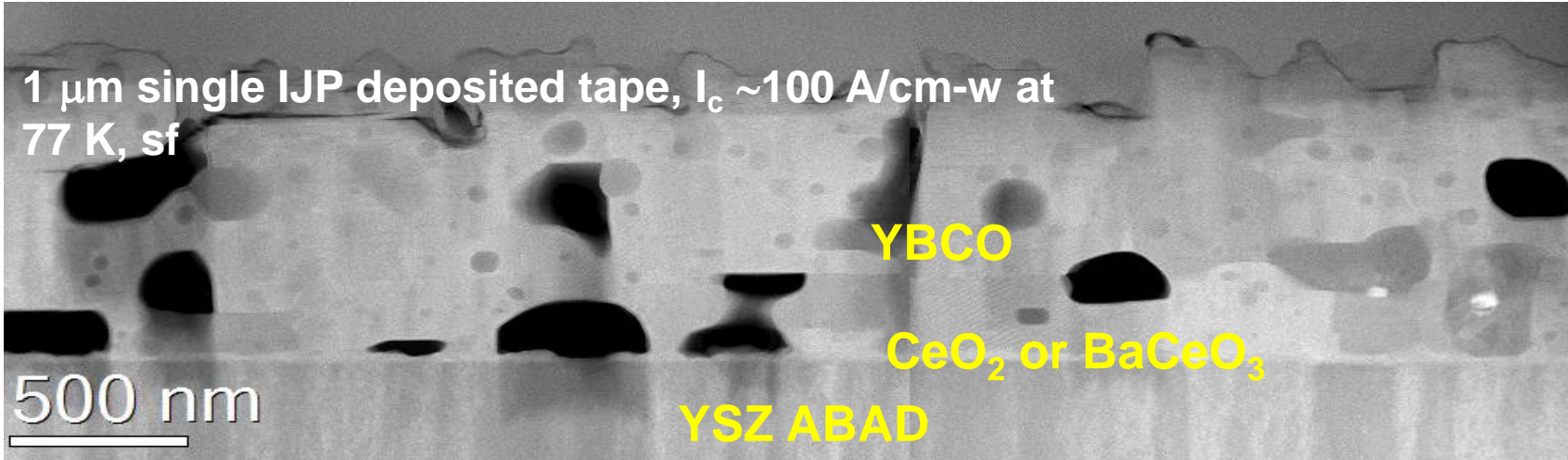
ICMAB



UAB
Universitat Autònoma de Barcelona



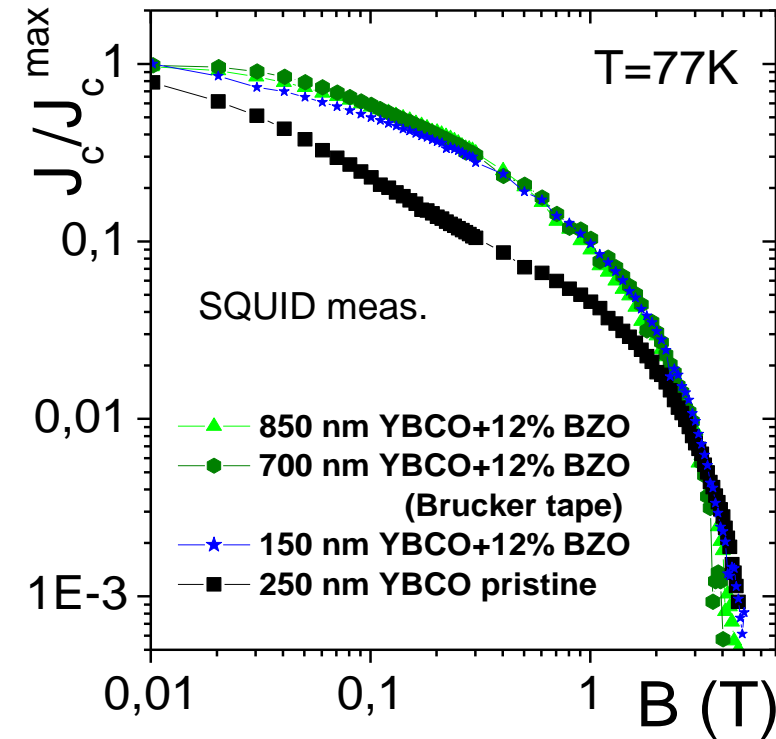
IJP single deposition on ABAD substrates



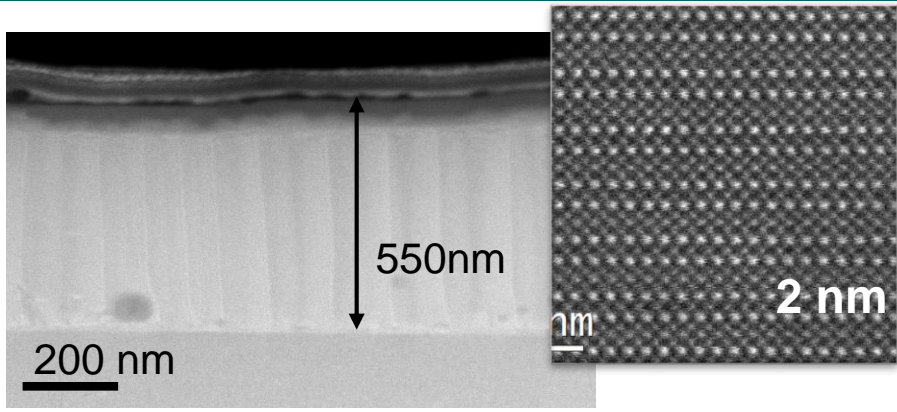
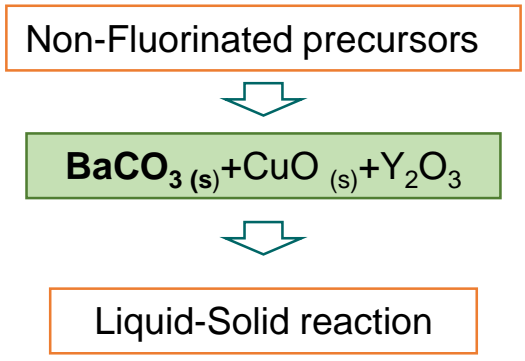
700 nm 12%M BZO on Bruker substrate

$J_c^{SF} = 1.4 \text{ MA/cm}^2$ at 77 K
Same dependence than in sc

Promizing results but still limited by pores in the matrix → further optimization is required

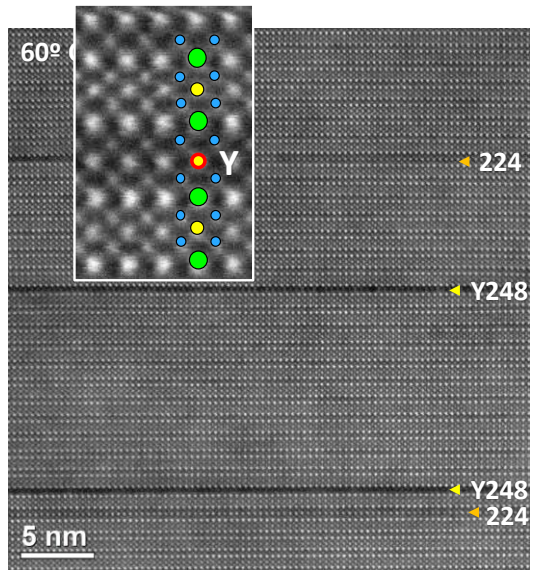


CSD-TRANSIENT LIQUID ASSISTED GROWTH (TLAG)

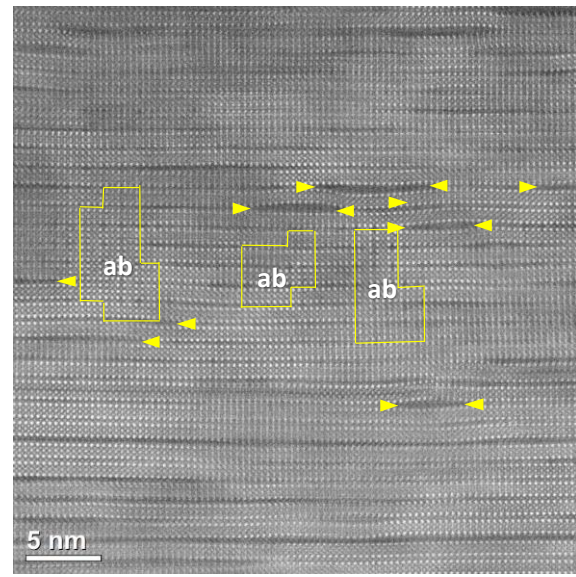


- Faster diffusion-> faster growth rate (x100)
- Highly simplified reactor
- More environmental friendly
- Highly epitaxial
- extremely low porosity. $J_c(77K) = 3 \text{ MA/cm}^2$

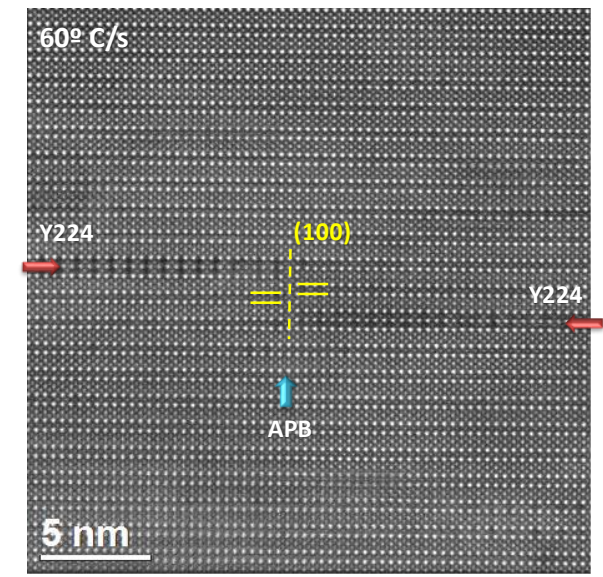
Growth process can strongly modify the nano(microstructure) of these films



Addition of a Y-Cu pervoskite block



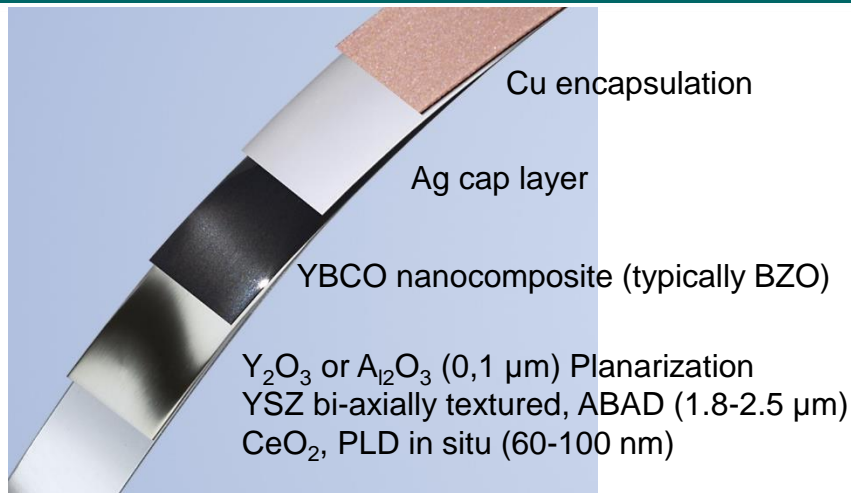
Nanoscale ab-grains



Antiphase boundaries

Opportunity to play with new pinning landscapes

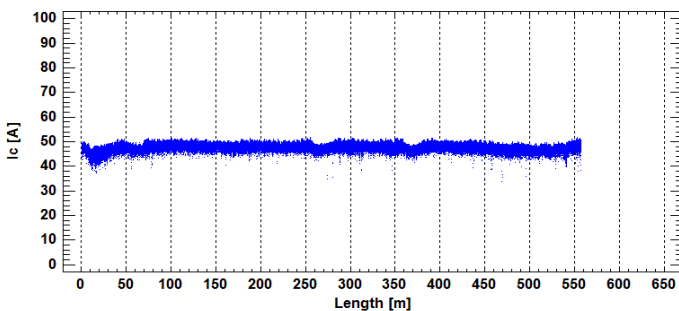




600 m long 4mm wide Cr-Ni SS (100μm)

- I_c Uniformity along 4mm wide wires at 77K

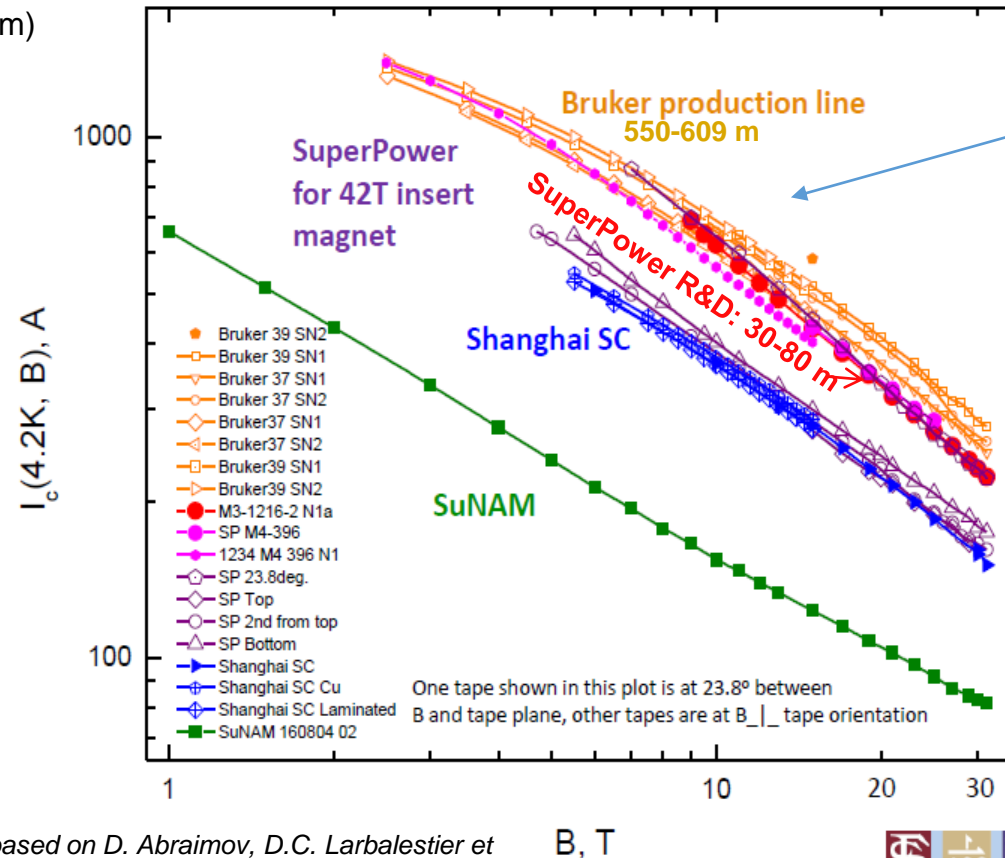
Reel-to-Reel hall-probe measurement of 4mm wide, 600 m long tapes along the entire tape length at 77K for defect detection and uniformity control



Courtesy of A. Usoskin based on D. Abaimov, D.C. Larbalestier et al. (NHMFL) WAMHTS-4 Barcelona in Feb. 2017

- Capability to process **4mm** wide HTS tapes with a max. single piece tape length of **600m**
- Capability to process **12mm** wide HTS tapes with a max. single piece tape length of **100m**

Nanocomposites fully implemented (600 m long tapes)



Bamboo-like nano-columns firework structure with very pronounced deviation from H//c



High I_c performance at ultra-high fields

NANOCOMPOSITES IN LAB. BUT ON-LINE IMPLEMENTATION IN A LATER STAGE

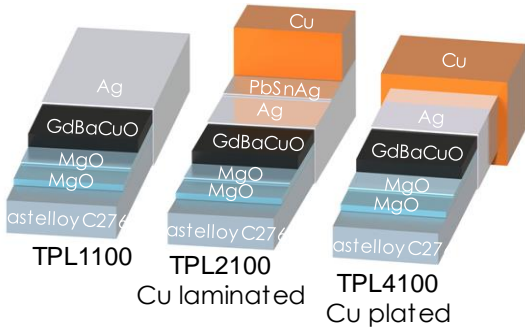
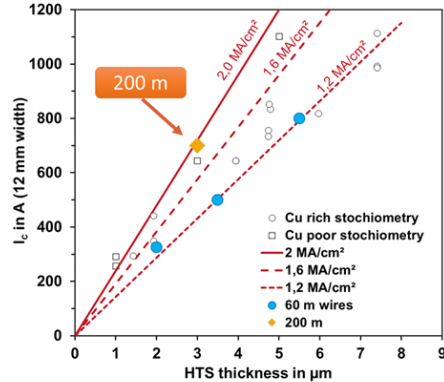
THEVA



Pilot line for industrial HTS wire production

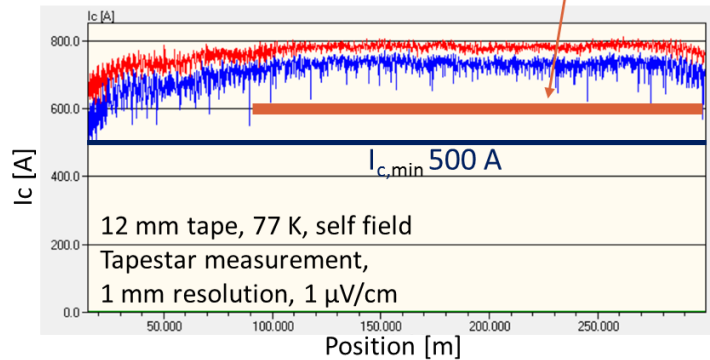
Capacity 150 km/yr
(@ 12 mm-width)

Typical production tape length: 300 m



different wire types

Over 200 m: $I_c \approx 700$ A, $I_{c,min} = 600$ A



Improved wire performance

PVD 2G CC

CSD 2G CC

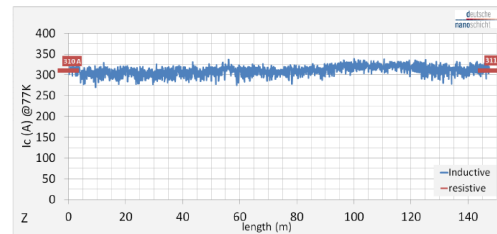
deutsche
nanoschicht

CSD for complete layer architecture
YBCO / CeO₂ / La₂ZrO₇ / Ni RABiT

- Length up to 500m
- Width 4-40mm
- Capacity >100km/a

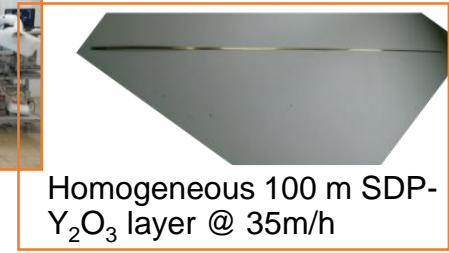
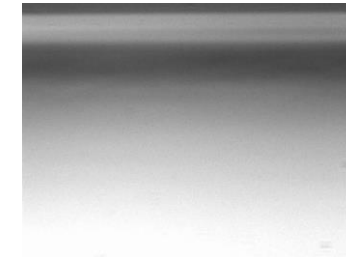


4x25m annealing furnace



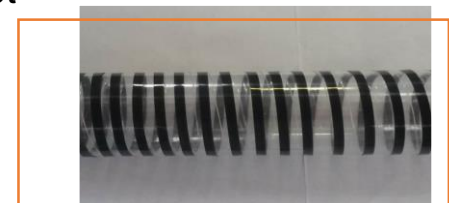
150mx10m, 310 \pm 10A (77K,sf)
Homogeneity <5%

OXOLUTIA



10 m CZO buffer @ 28 m/h

Reel-to-reel IJP pilot plant all CSD



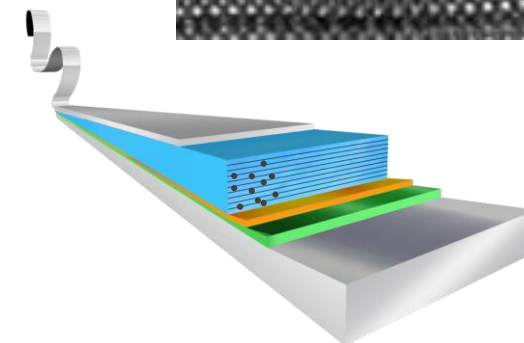
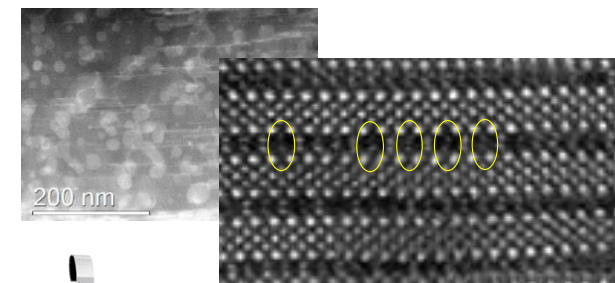
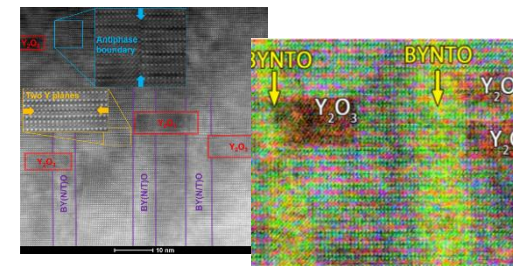
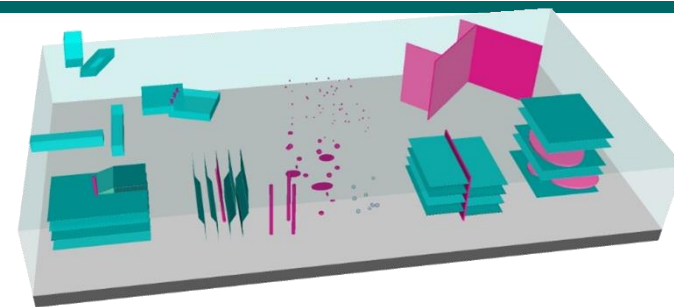
10 m of YBCO

Bruker & SuperOx substrates



CONCLUSIONS AND PROSPECTS

- Large knowledge in the correlation between vortex pinning and APC & Natural Defects in ReBCO films has been achieved allowing to identify the best pinning landscapes
- PLD: Mixed of random and correlated defects: Better pinning performances for most regimes of magnetic field and temperatures.
- CSD: Mixed spontaneous segregated NP and preformed NP: Good pinning performances with combination of weak and strong pinning centers
- PLD & CSD thick nanocomposite films have been integrated on technical substrates
- New approaches for fast growth rates & long length CC nanocomposite development represent the major present efforts



COLLABORATORS : NANOSTRUCTURE ENGINEERING

ICMAB-CSIC:

X. Obradors, T. Puig, M. Coll, J. Gázquez, X. Granados, S. Ricart, F. Vallès, B. Mundet, Z. Li, R. Guzman, C. Pop, B. Villarejo, F. Pino, J. Banchewski, L. Soler, J. Jareño, A. Stangl



ENEA:

G. Celentano, A. Augieri, F. Rizzo

UCAM:

J. Driscoll, A. Kursomovich

IFW-Dresden:

R. Hühne, P. Pahlke, M. Sieger

KIT-Karlsruhe:

B. Holzapfel, J. Hänisch, M. Erbe, P. Cayado

TU Wien:

M. Eisterer, M. Lao

UGENT:

I. Van Driessche, K. Keukeleere

U. Antwerpen:

G. Van Tendeloo, A. Meledin

Bruker:

A. Usoskin, K. Schlenga

D-Nano:

M. Bäcker, M. Falter

THEVA:

M. Bauer, W. Pruseit

Oxolutia:

A. Calleja, XR. Vlad, M. Vilardell



CATALONIA

